

Mineralogical Characterization of the Early Silurian Shales as Encountered in Southern Tunisia

Mohamed Soua

Department of Geology, University of Tunis El Manar, Campus Universitaire, Tunis, Tunisia

elmohology[at]yahoo.fr

Abstract: This study presents whole rock and clay fraction analysis of the Silurian Argiles Principales Formation from southern Tunisia Berkine Basin. The organic-rich Hot Shale interval is marked by prevalent illite amount compared with the overlying succession. However, enhanced preservation of widespread enrichment of kaolinite that marks the overlying shales with small variability of chlorite and I/S is being noted. The predominance of the kaolinite on top of the 'Hot shale' Member is interpreted as being derived chiefly from acid conditions capable of generating processes of preservation resulting from intense feldspars decomposition under strong acid water drainage. The elevated organic matter preservation is probably inferred from increased primary productivity and redox conditions testified by the presence of small-sized pyrite framboids and probable microbial mats at the bottom water interface during subsequent burial of the Silurian sediments. This may indicate shallow and calm anaerobic environment resulting from activity of sulfate-reducing bacteria during the early Silurian. This has been tied to an echo of intensified oxygen minimum zone expansion along the Gondwana margins during global to regional anoxic mass-extinction events (Sandvika, Ireviken, Mulde and Lau). In this paper, we present new nomenclature related to the studied Silurian shales in southern Tunisia.

Keywords: Argiles Principales Formation, Clay mineralogy, Southern Tunisia, Silurian Isotopic Events

1. Introduction

1.1. General Overview

Although, the early Silurian strata do not crop out in southern Tunisia, they have been encountered by plenty of wells in Berkine and Jeffara basins (Fig.1). Previous studies conducted on the 'Argiles Principales' Formation have chiefly evaluated organic geochemical and palynological

characteristics of the early Silurian source rock. This has been achieved as a result of a generalized evaluation with emphasis on the regional distribution of the organic-rich and graptolitic black shale facies along the North African margin including Libya, Tunisia, Algeria and Morocco (e. g. Jaeger et al., 1975; Massa, 1985; Boote et al., 1998; MacGregor, 1998; Lüning et al., 2000; Craig et al., 2008; Vecoli et al., 2009; Loydell et al., 2009; Rezouga et al., 2012; Soua, 2014; Gambacorta et al., 2016).

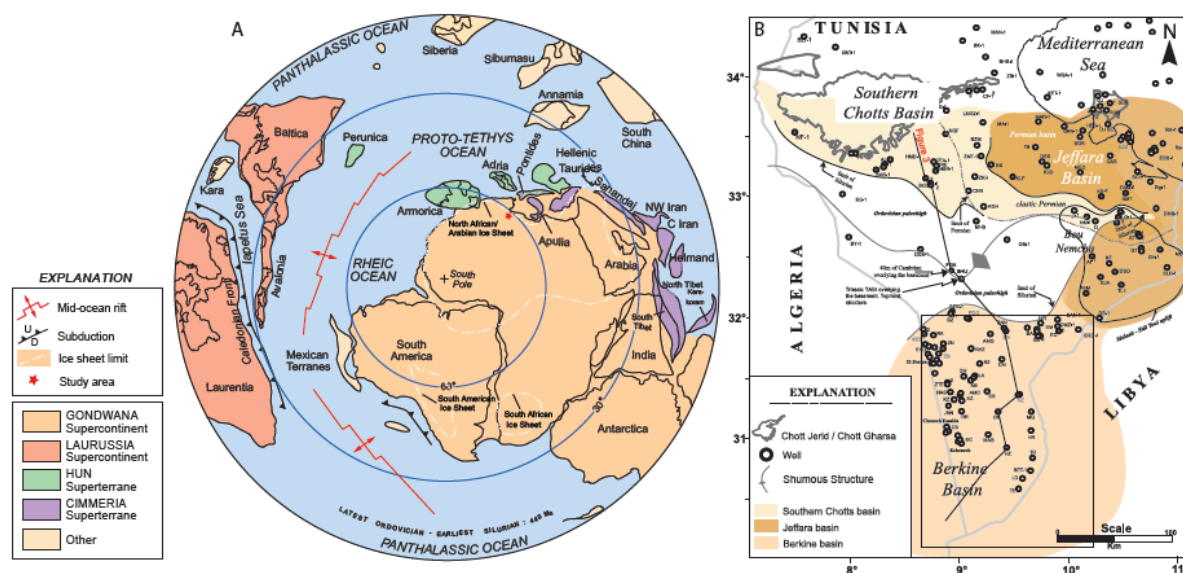


Figure 1: Paleogeographic reconstruction at the earliest Silurian and presentation of the study area. **A.** Paleogeographic reconstruction of the earliest Silurian (modified after Cocks and Torsvik, 2002; Ruban et al., 2007). Latest Ordovician glacial reconstruction and advancement over regions of Gondwana is due to Le Heron et al. (2009). The reconstruction shows Gondwana supercontinent, Baltica, Laurentia and few other terranes along with three main palaeo-oceans including the Proto-Tethys (comprising the Panthalassic Ocean), Iapetus and Rheic Oceans. **B.** The three main sedimentary basins characterizing the southern Tunisia: southern Chotts, Jeffara and Berkine basins (Soua, 2014)

The radioactive organic-rich Hot Shale facies produce 12.15% TOC in average, while the overlying Argiles Principales shales account typically for 0.5%TOC being considered as organically lean (Rezouga et al., 2012; Soua, 2014).

Volume 11 Issue 10, October 2022

www.ijsr.net

Licensed Under Creative Commons Attribution CC BY

Conversely, these organic-rich black shales are commonly labelled 'Hot Shales' (e. g. Lüning et al., 2000) or radioactive shales (Jaeger et al., 1975) and covered multiple basins of the Gondwanian margins (e. g. Lüning et al., 2000; Loydell et al., 2009; Soua, 2014). Furthermore, these organic-rich and laminated succession is interpreted as being deposited during severe conditions of anoxic event (e. g. Lüning et al., 2000; Soua, 2014; Gambacorta et al., 2016). The early Silurian stage has recorded the preservation of a worldwide important organic carbon amount as a response to the prevailing paleoceanographic conditions at that time (Kaljo et al.1997; Lüning et al., 2000; Saltzman 2001; Calner, 2008; Cramer et al., 2012; Loydell et al., 2013; Cooper et al., 2014; Crampton et al., 2016; Danielsen et al., 2019; Bowman et al., 2019). In addition, the Hot shale source rock in southern Tunisia (Berkine and Jeffara basins) is the main hydrocarbon generator for most of Paleozoic reservoirs (e. g. Soua, 2014).

However, very rare studies have been published on the mineralogical composition of the early Silurian shales (e. g. Hassan and Massa, 1975; Soua, 2014; Gambacorta et al., 2016), which is considered to be one of the important key to provide a reliable interpretation in terms of depositional environment (Dickinson et al., 1983; McLennan et al., 1993; Roser and Korsch, 1988; Soua, 2019).

1.2. Study area

In the subsurface of Southern Tunisia, the Silurian is unconformably overlying the top of the glacial valley-filled along with glacio-fluvial and glacial marine sandstones of Jeffara Formation. The lowermost Silurian is either absent or forms part of the "Dalle de M'Krata" which may be indicative of the Silurian sea transgression along North Africa (Kiltzsch, 1969, Legrand.1981; Memmi et al., 1986; Wennekers et al., 1996; Luning et al., 2000; Guiraud et al., 2005; Craig et al., 2008; Abuhmida, 2013; Soua, 2014). Legrand (1981) mentioned that the M'krata sandstone bed (spelled M'kratta) form the upper part of the Ramada sandstones which overlies El Golea shales Member of the Hassi El Hadjar Formation in Algerian Central Sahara (Oued Mya, Oued Saret and Oued El Biod). This level could be the equivalent of the Iyadhar Formation, which is defined in the Mourzouk Basin in Libya by Massa and Jaeger (1971). The topmost terms of the Silurian are absent due to the epeirogenesis of early Caledonian age (Massa and Beltrandi, 1975; Luning et al., 2000; Soua, 2014).

The main stratigraphic data are due to Bonnefous (1963) Jaeger et al. (1975) and Vecoli et al. (2009) who established a zonation based on graptolites and chitinozoans.

The type section of the "Argiles Principales" Formation is located at well Sidi Toui (ST1; see Figure 1B, for location) in Jeffara, southwards Ben Guerdan with about 174 m thick. This Formation was first defined by Massa and Jaeger (1971) in Libya, in the so-called Ghadames basin. Then, Jaeger et al. (1975) were able to establish a good zonation thanks to the graptolites assemblages.

The total thickness of the early Silurian shales (Argiles Principales Formation) in southern Tunisia is generally

controlled by the Caledonian uplift and erosion, which may have affected both original and post-erosional thickness (Soua, 2014). The Caledonian tectonic event is most probably the main responsible for frequent angular unconformities overlying the Argiles Principales Formation. These tectonic instabilities are believed to be the one of the major causes responsible for the partial to total erosion of this sequence in the northernmost part of the basin, i. e. Jeffara and northern Berkine Basin (e. g., Boote et al., 1998; Guiraud et al., 2005).

The accumulation and preservation of the organic material amount during end-stage episodes of glaciation and deglaciation, related to the ice-sheet glacial retreat, which occurred due to specific paleoceanographic conditions still in debate by some authors, from which different paleoceanographic models have been presented (e. g. Luning et al., 2000; Vecoli et al., 2009; Moreau, 2011; Melchin et al., 2013; Loydell et al., 2013; Soua, 2014; Gambacorta et al., 2016).

In this paper, whole rock and clay mineralogy investigation is presented from five wells (EPB-1, CEM-1, SET-1, AMC-1 and HWA-1) located in southern Tunisia. The data is combined to mineral wireline data acquired for well HYT-1 and isotopic organic carbon content measured for the same section by Vecoli et al. (2009). Our aim is to reconstruct the conditions under which the early Silurian shales have been deposited and try to contribute to the general understanding of the related paleoenvironmental changes of this period of time.

2. Geological Setting

2.1. Background overview

During the latest Ordovician to earliest Silurian time, the global continental reconstruction was most probably composed chiefly of Gondwana supercontinent, Baltica, Laurentia and few others (Fig.1A). Three main palaeo-oceans separated the aforementioned supercontinents comprising the Proto-Tethys (which includes the Panthalassic Ocean, located in the north of the Proto-Tethys), Iapetus (separated Laurentia and Baltica) and Rheic (closed during mid-Carboniferous between northwest Africa and southeast North America due to the Hercynian Orogeny) Oceans (Ziegler et al., 2001; Stampfli and Borel, 2002; von Raumer et al., 2002; Scotese, 2004; Ruban et al., 2007).

2.2. Southern Tunisia

During this period, southern Tunisia including Berkine Basin belongs to the Gondwana supercontinent. This large supercontinent covers most of the Silurian land masses including Africa, South America, Florida, Arabia, India, Antarctica and most of Australia (Cocks and Torsvik, 2002; Stampfli and Borel, 2002; Ruban et al., 2007; Soua, 2014; Fig.1). It was generally associated with the southern pole, located roughly in nowadays within North to western Africa during the latest Ordovician-earliest Silurian (Scotese et al., 1999; Cocks and Torsvik, 2002; Ruban et al., 2007; Le Heron et al., 2009; Soua, 2013, 2014). Late Ordovician ice sheets grew up to cover the northern part of Gondwana

platform including North Africa and Arabia (e. g. Ghienne et al., 2007; Le Heron and Craig, 2008). The ice sheet affected North African basins including Berkine, Illizi, Hamra, Kufra, Ahnet, and Taoudeni (e. g. Beuf et al., 1971; Fabre, 1988; Ghienne and Deynoux, 1998; Luning et al., 2003).

The uppermost glacial and sub-glacial fluvial channels and paleo valleys in southern Tunisia are represented by the “Dalle de M’kratta” (see Soua, 2013 for discussion). This sequence overlies commonly glaciogenic shallow to offshore marine micro-conglomeratic shale and sandstones of Jeffara Formation (Jaeger et al., 1975; Memmi et al., 1986; Ben

Farjani et al., 1990; Carr, 2002; Guiraud et al., 2005; Vecoli et al., 2009; Soua, 2013; Fig.2). This glacial climatic event was associated or slightly trailed by the Taconic tectonic event, which characterizes generally the Ordovician–Silurian transition. The Late Ordovician icecap melting induced the early Silurian sea-level rise, inducing an important organic-rich shale sedimentation above the basal Silurian paleo valley-fills covering most of the North African and Arabian basins, containing abundant pyrite and graptolites (Luning et al., 2000; Hallett, 2002; Guiraud et al., 2005; Le Heron and Craig, 2008; Loydell et al., 2013; Soua, 2014).

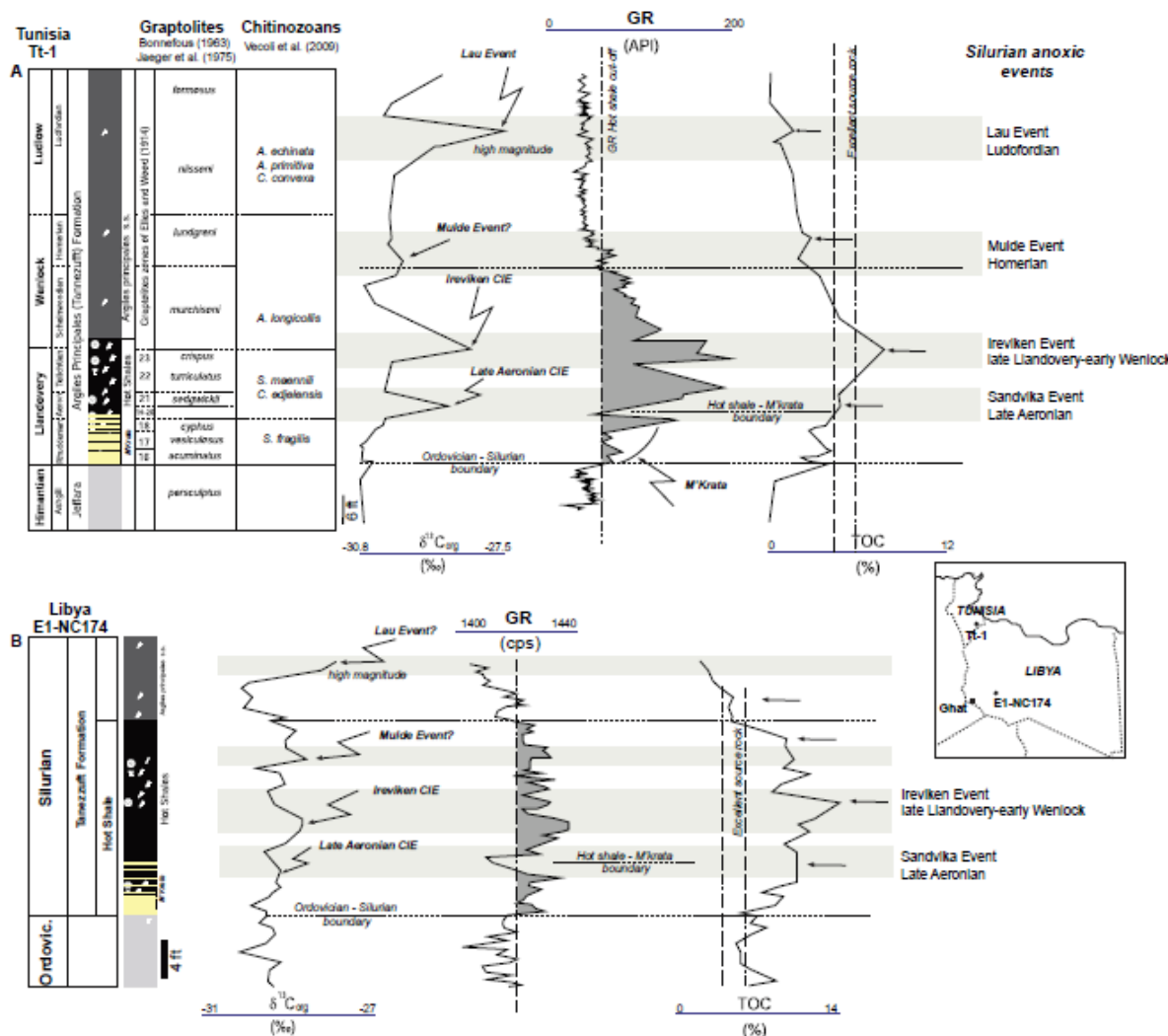


Figure 2: Stratigraphic vertical variation and a correlation attempt of $d^{13}C_{org}$ in relation with Gamma ray (GR) and TOC in southern Tunisia and south-eastern Libya. The $d^{13}C_{org}$ are interpreted in terms of Silurian bioevents. GR values cut-off are set for hot shale indication (shaded color in grey) and TOC are interpreted in terms of source rock potential. Arrows indicate probable peaks related to Sandvika, Ireviken, Mulde and Lau events. **A.** Vertical variation of $d^{13}C_{org}$, GR and TOC in well Tt-1 (southern Tunisia). **B.** Stratigraphic variation of $d^{13}C_{org}$, GR and TOC in well E1-NC174 (south-eastern Libya)

Some authors (e. g. Troudi et al., 2012), still confuse the elevated gamma ray response of the Haj Brahim Formation (=Fegaguira: late Silurian-early Devonian; Soua, 2014) located in Southern Chott Basin with the typical early Silurian Hot Shale in southern Tunisia without taking into account the palynological investigations made by Dummond and Rasul (1985), which confirmed the late Silurian-early Devonian age in the southern Chott basin.

The study area is bounded towards the North by an E-W uplift structure called Touggourt-Talemzane-PGA-BouNamcha (TTPB) structure by Soua (2014). Recent drilling programs has shown that the top of the structure is present in Tunisia and has been penetrated by well SHU-1 (Shumus-1) in which the Triassic sandstones lie directly on the Precambrian basement (Figs.1 and 3).

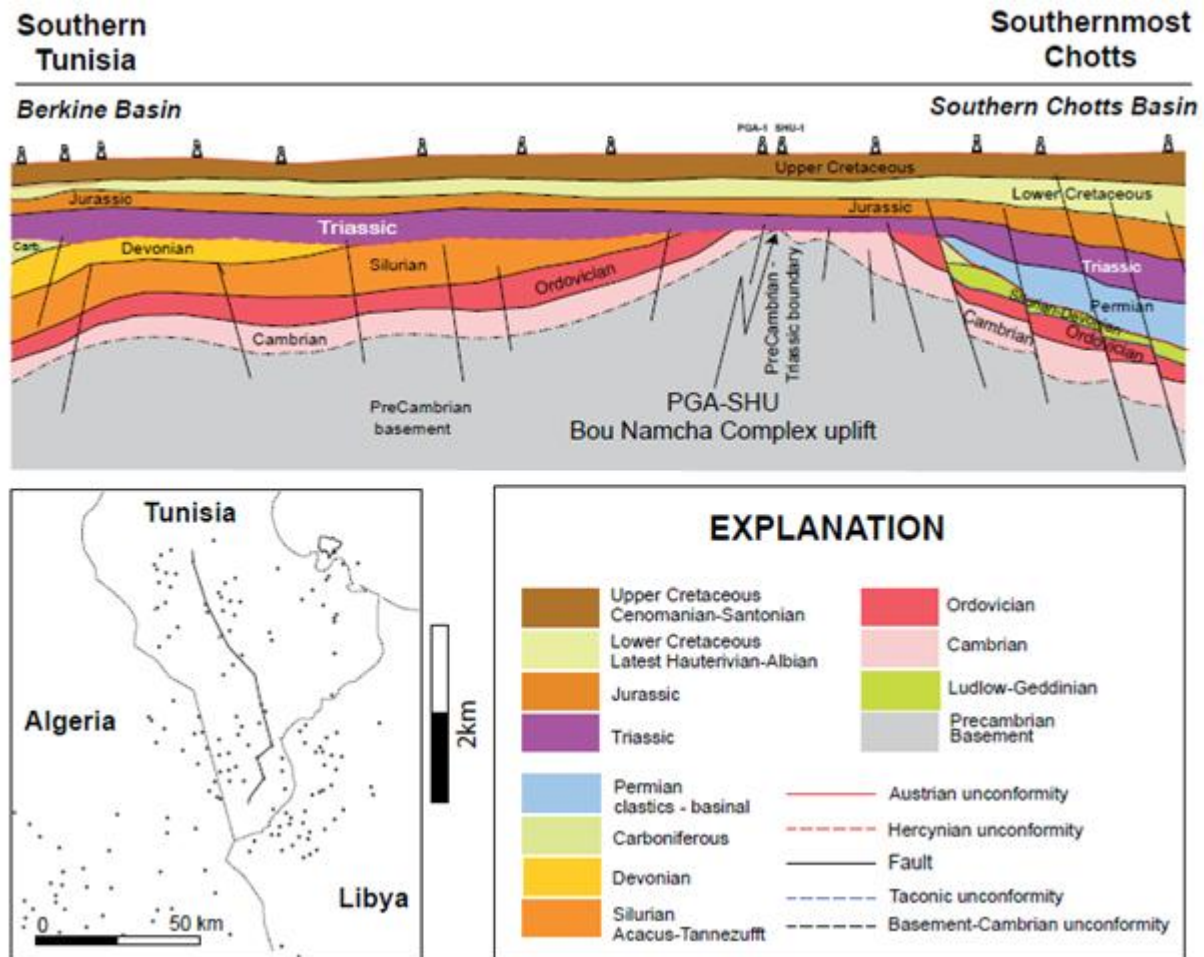


Figure 3: Proposed geoseismic cross sections showing the main structural styles affecting the Berkine and Jeffara Basins. Modified from Soua (2014)

2.3. Lithostratigraphy

Soua (2014) argued that the organic-rich early Silurian hot shale distribution may have represented anoxigenic minimum zone (OMZ) impingement onto the southern Tunisia (Berkine Basin).

In general, it is commonly known that the Hot Shale interval is composed of two distinct units interestingly deposited during a eustatic sea-level fall (Loydell et al., 2013). A lower unit, which is generally made of silty bioclastic to peloidal bioclastic wackestone and packstone with scarce quartz, grains bearing diversified graptolite assemblages (Jaeger et al., 1975). This unit progrades to organic-lean and thinner bioclastic limestone alternating with shaly limestone and fine sandstone towards the west (Memmi et al., 1986). However, the upper unit consists generally of mudstone to wackestone delivering diversified graptolites along with chitinozoans (Vecoli et al., 2009). This sequence passes to carbonate towards the southwest. Daniels and Emme (1995) reported a single 16% TOC value from the El Bormafeld (Soua, 2014). The paleogeography of the early Silurian black shales level in Southern Tunisia is strongly associated with the deposition setting with the proximal settings are being marked by important carbonate deposition associated with bioclast while distal settings are generally dominated by marls and shale. It is in this setting where organic-rich marls

highlight the significance of anoxic and dysaerobic environments.

3. Analytical procedure and methods

An early to late Silurian stratigraphic succession has been sampled from wells AMIC-1, CEM-1, EPB-1, HWA-1; SET-1 and OZ-1 along Berkine basin in southern Tunisia (See Figure 1 for location). A total of 115 cuttings were sampled including the 'Hot Shale' Member along with the remaining 'Argiles Principales' Formation. These cuttings were subject of mineralogical analyses including whole-rock and clay fraction along with ESEM analyses.

Wireline log data including Spectral Gamma Ray (SGR), SpectroLith logging data, etc. for wells HYT-1, AMC-1 and HWA-1 have been utilized to estimate organic richness, paleoredox, primary productivity and mineral composition.

3.1. Whole rock mineralogy

The samples were cleaned from oil-based mud, then crushed using a mortar and pestle and finally sieved to mesh 125 μm in order to be homogenized. Some of the data has been previously published in Soua (2014).

A total of 115 cutting samples related to wells AMIC-1, CEM-1, EPB-1, HWA-1 and OZ-1 were analyzed for whole

rock mineral composition using X-ray diffraction method (XRD) utilizing a PANalytical X'Pert PRO instrument (operating at 45 kV and 40 mA and equipped with a CuK α) in the Faculty of Science at Tunis. The goniometer was step-scanned from 5° to 50° 2-theta in steps size of 0.02°. Rietveld full-pattern fitting method was used to quantify the identified crystallographic planes related minerals described by Young (1993) and Grunsky et al. (2013) based on full-profile fitting procedures. The semi-quantification has been possible using X'Pert High-Score Plus (PANalytical) software. Data from well SET-1 has been taken from Gambacorta et al. (2016).

3.2. Clay mineralogy

The clay fraction process is employed for the determination of crystalline clay size (<2 microns) components. Samples were crushed to <2 microns fraction then decalcified with 0.5M HCl and distilled water. After being processed for sonification and centrifugation, the clay fraction is oriented on a glass slide.

After the clay slides are being analyzed in an air-dried state, the samples are also analyzed after being exposed to ethylene glycol (EG) fumes and heated to 350 °C. The exposition to EG causes the spacing of the basal planes to increase for expandable clay minerals in order to allow easy differentiation between illite, smectite, and ordered and randomly interstratified (illite-smectite) clay minerals. The accuracy strongly depends on the specific composition, homogeneity and crystallinity of the samples. Analysis was carried out with goniometer is being set on step-scan from 3° to 35° 2-theta in steps size of 0.02°.

3.3. ESEM microscopy

Selected samples were analyzed and photographed using an Environmental Scanning Electron Microscope (ESEM) in ETAP. Samples were initially mounted on aluminum stubs and covered with carbon-conductive adhesive tape. Conditions performed were generally in high and low vacuum and accelerating voltage.

3.4. SpectroLith logging tool

SpectroLith logging has been run for well HYT-1 (Hayatt-1), which penetrated the early Silurian succession (Soua, 2014). This logging technology provides data of geochemical elemental concentrations acquired through Elemental Capture Spectroscopy (ECS) tool including, but not restricted to, weight percentages (%) of Al, Ca, Fe, Si, S and Ti along with mineral-modelled composition of carbonate, clay, pyrite and quartz volumes (Lewis et al., 2004; Cluff and Miller, 2010; Soua, 2014).

3.5. Biostratigraphic calibration

Bonnefous (1963) reported *Climacograptus extremus* in wells Lg-3 and ST-1 that range in the Upper Rhuddanian *Cyphus* Zone. He also reported *C. rectangularis*, ranging from *acuminatus* to *gregarious* along with *Rhaphidograptus toernquisti*, which first appearance occurs in the *vesiculosus* indicating a Rhuddanian age (Soua, 2014).

Davidson et al. (2000) assigned early Llandovery age to the Hot shale unit of the Tannezuft Formation in Murzuk Basin. It has been also reported as Rhuddanian age by Hallet (2002). In general, Graptolites stratigraphy shows a Rhuddanian to earliest Aeronian age in both Tunisia and Libya (Jaeger et al., 1975; Memmi et al., 1986; Štorch and Massa, 2006; Vecoli et al., 2009; Paris et al., 2012; Loydell et al., 2013; Butcher, 2013).

In general, a Rhuddanian age has been assigned for the radioactive high gamma ray marker in southern Tunisia based on graptolites (early Llandovery) in several wells (including Tt-1, CEM-1, AMC-1, HWA-1, EB-1, SET-1) (Bonnefous, 1963; Jaeger et al., 1975; Massa, 1985; Memmi et al., 1986; Ben Ferjani et al., 1990 and Vecoli et al., 2009; Soua, 2014; Fig.2). This biostratigraphic level can range to the *sedgwickii* graptolite Zone (Jaeger et al., 1975; Vecoli et al., 2009) in southern Tunisia, indicative of Aeronian age. The radioactive high Gamma ray marker level include in general the *murchisoni* and *rigidus* graptolites zones, with the latter can range above the hot shale interval. These assemblages are indicative of early Wenlock (Sheinwoodian) (Jaeger et al., 1975; Memmi et al., 1986; Vecoli et al., 2009). According to Vecoli et al. (2009) acritarchs species including *Ammonidium microcladum*, *Oppilatala sp.*, *Tylotopalla sp.*, *Quadratum fantasticum* (Telychian–Wenlockian age) range just above the radioactive high gamma ray interval. While chitinozoans *Spinachitina fragilis*, *Spinachitina maennili*; *Conochitina aedjelensis aedjelensis* and *Angochitina longicollis* diagnose for Rhuddanian to lower Sheinwoodian age (see Soua, 2014 for discussion). Unfortunately, most of cored sections with regards to the Silurian hot shales in southernmost Tunisia have not been subject to advanced biostratigraphic analysis and their related palynomorphs distribution still remain unclear and need more investigation. The reason why, correlation of the subject interval between Bir Ben Tartar, Kasbah Leguine and Sidi Toui type and reference sections has been taken as an option.

4. Results

The early Silurian “Argiles Principales” in southern Tunisia starts with very thin pyritic fine sandstone marker known as “Dalle de M'Krata” which may contain in general silty and pyritic shales with sporadic alternations of carbonates evolving laterally into shales towards the basinal setting. This level is overlain by highly radioactive shales with high-magnitude Gamma-ray order reading set as the marker for early Silurian ‘Hot Shale’ interval. This level pass gradually into organic-lean shales and silt alternation of the ‘Argiles Principales’ Formation *sensu stricto* (s. s.). The Hot shale Member was deposited within an anoxic environment with preservation of type II organic matter. However, the overlying fine to very fine grained material dominated by shales along muddy fine grained levels and silts and sandstones of the ‘Argiles Principales’ Formation have been affected by tidal currents along with storm waves and tidal inlets.

4.1. Whole rock and clay mineralogy

Figures 4 (A and B) show the bulk and clay mineralogical data presented in this study.

The XRD results indicate that the samples consist primarily of quartz, kaolinite and illite/mica as major mineral constituents. K feldspar (microcline) and plagioclase (albite) are not significant with amount is less than 5% in average. Other minerals reported include calcite, dolomite, chlorite, anhydrite, halite and hematite. Clay minerals results show that the analyzed samples report illite, mixed layer illite/smectite (I/S), kaolinite, and chlorite, which have been commonly described from Argiles Principales Formations. In general, they occur mainly as grain coats, pore-fills and laminae. It is noted that no discrete smectite

(montmorillonite) is identified in the studied samples. Figure 5 shows that the accessory minerals are present within finely laminated mudstones. They comprise in general a number of grain components including very fine quartz, mica, clays, small sized framboids of pyrite and scarce carbonate fragments (Fig.5 A, B, C). These are associated with laminated irregular features, interpreted as being presence of microbial mats (Fig.5B). All samples show poorly interconnected and relatively poorly preserved porosity (e. g. Fig.5D).

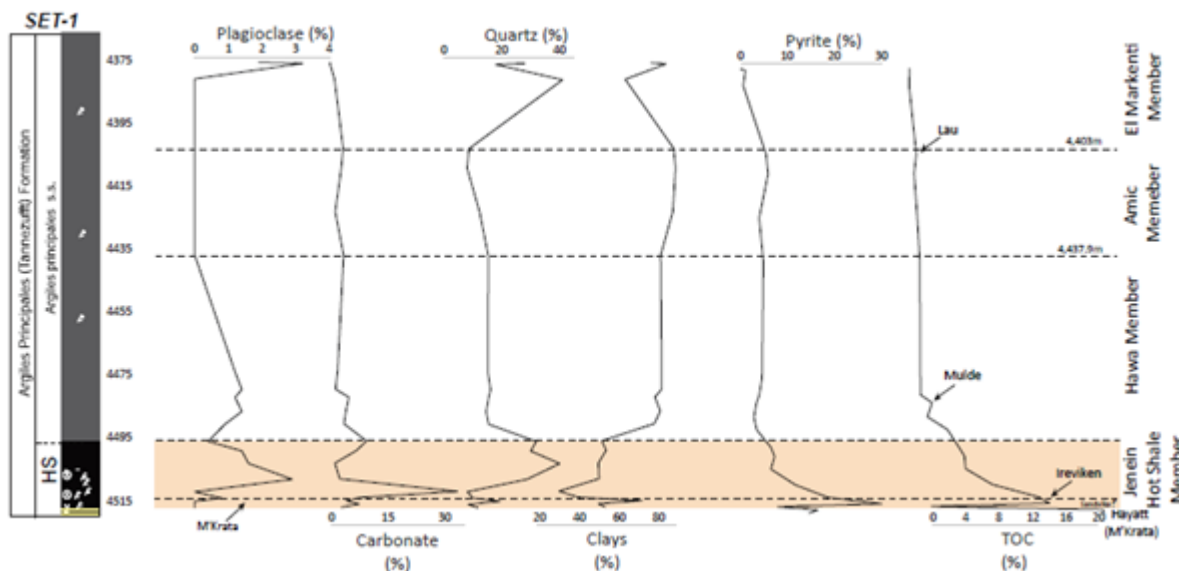


Figure 4A: Bulk mineralogy analyzed in well SET-1. Members discussed in the text are shown along the figures in relation with the mineral trends.

Illite/mica along with quartz are the main mineral constituents (38.3% and 32.1% respectively at well SET-1; Fig.4A) in M'Krata Member beds with emphasis on important amount of pyrite (16.5%) and calcite (around 8%), whereas a remarkable increase in illite/mica coincident with a slight drop in quartz (around 55% and 23%, respectively) mark the hot shale Member. Kaolinite content around 5% in M'Krata and increases slightly to 11% in overlying hot shale interval. Feldspar are mostly absent in the aforementioned intervals (Fig.4A). The overlying sequences in Argiles Principales Formation are marked by three distinct members (see later in the text), in which proportions of the mineral

constituents vary significantly. Above the hot shale Member, illite/mica and kaolinite are the main mineral phases, which constitute the bulk mineralogy. Quartz varies and slightly decreases. In the shaly intervals it drops to ca.9% while in the sandy/silty levels it constitutes less than 30%. K feldspar and plagioclase are higher than in M'Krata and hot shale levels but do not exceed 10% in total. Pyrite significantly drops down from more than 16% in organic rich intervals to less than 1% in Argiles Principales. s. interval. For instance some samples yielded the presence of Barite (Fig.6). This latter mineral is associated with the drilling additives in this study (see Souza, 2019).

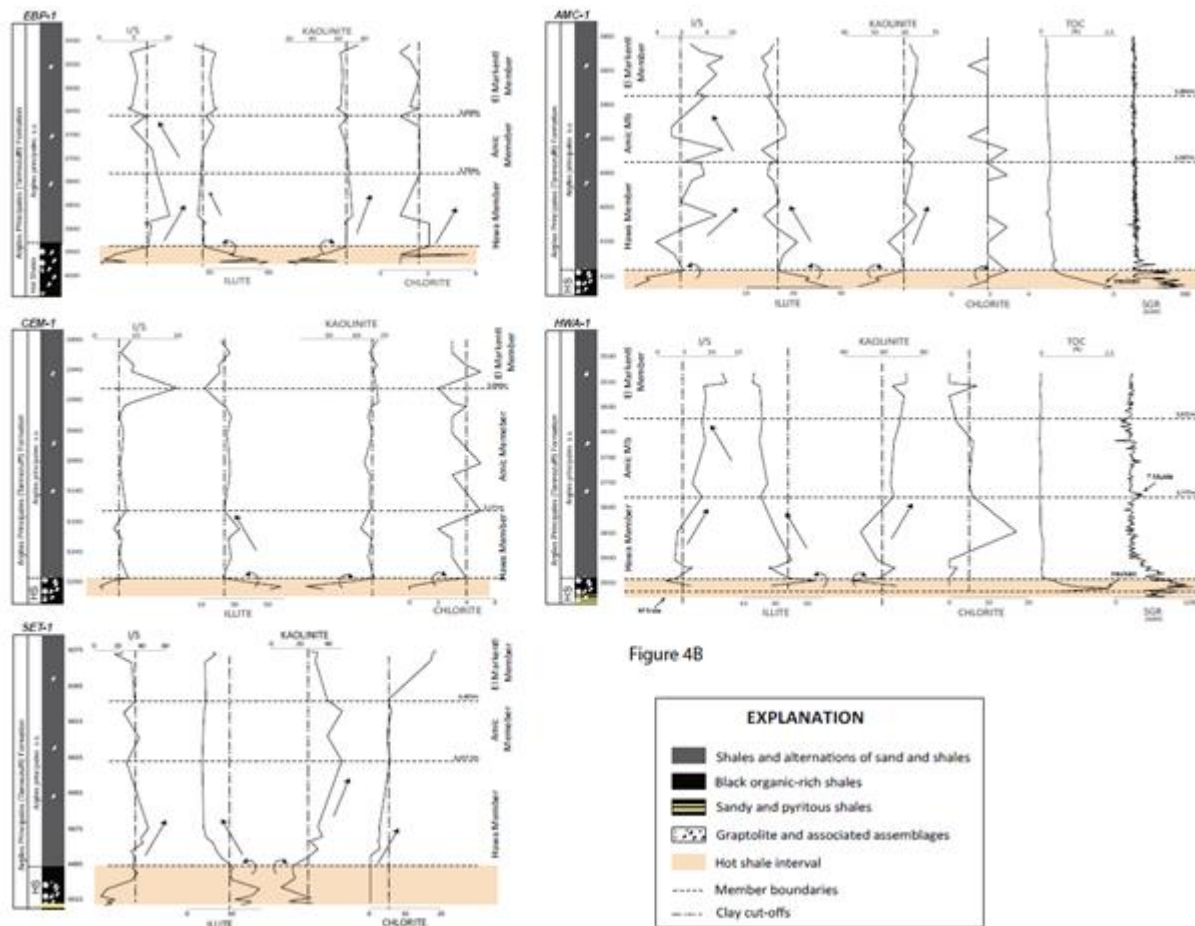


Figure 4B: Clay mineralogy processed in wells EPB-1, CEM-1, SET-1, AMC-1 and HWA-1. Members discussed in the text are shown along the figures in relation with the mineral trends.

Clay mineral assemblages consist essentially of illite, I/S mixed-layers and kaolinite (Fig.4B). Illite content exceeds 70% in both M’Krata and hot shales members. Kaolinite increases slightly at hot shale interval, while I/S mixed-layers form more than 15% of the clay assemblages in M’Krata Member. In the overlying sequences and just above the limit of the high radioactive shales level, kaolinite becomes the dominant clay mineral exceeding 60% of the

total clay fraction in wells CEM-1, AMC-1, HWA-1 and EPB-1. The highest values for kaolinite are observed along well EPB-1 in the shaly interval (Fig.4).

Figure 6 illustrates selective whole rock and clay-sized fraction XRD patterns which represent the main identified minerals/clay minerals in this study.

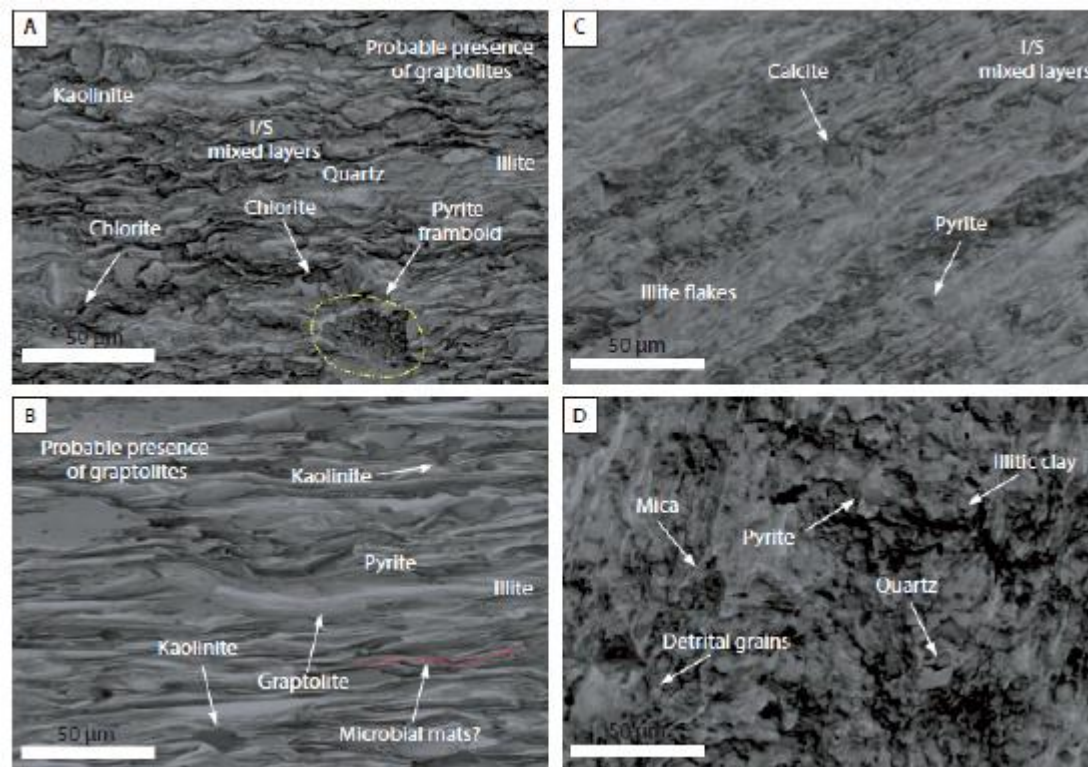


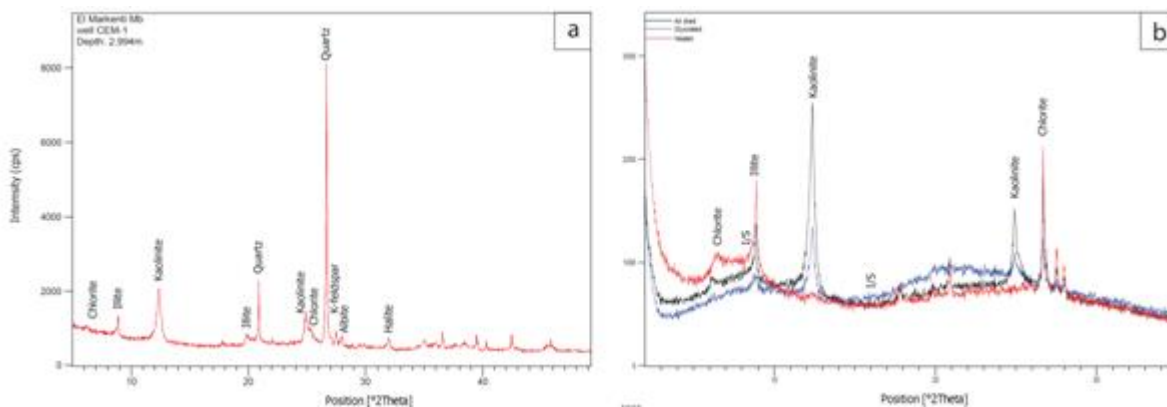
Figure 5: Selected scanning electron micrographs of lower Silurian shales southern Tunisia. **A** and **B** taken from levels above the hot shale and attest the dominance of kaolinite over illite, mixed layers I/S and chlorite. Pyrite framboids are frequent along with microbial mats-like and graptolite. **C.** Hot shale member. **D.** M'Krata member

4.2. Lithostratigraphy and definitions

Figure 4 shows that the Argiles Principales Formation is subdivided into members according to the mineralogical variation along the early Silurian stratigraphic succession. As argued above, the basal part of the Formation is mainly consisting of the M'Krata silty and carbonaceous interval overlain by the high radioactive Hot Shale interval. The

overlying Argiles Principales. s. is subdivided into three members: Hawa, Amic and El Markenti members (Fig.7).

The M'Krata Member is basically characterized by low plagioclase along with a drop in clay content and presence of an important amount of pyrite. The high quartz content is probably due to biogenic silica secreted by siliceous microfossils (Soua, 2014).



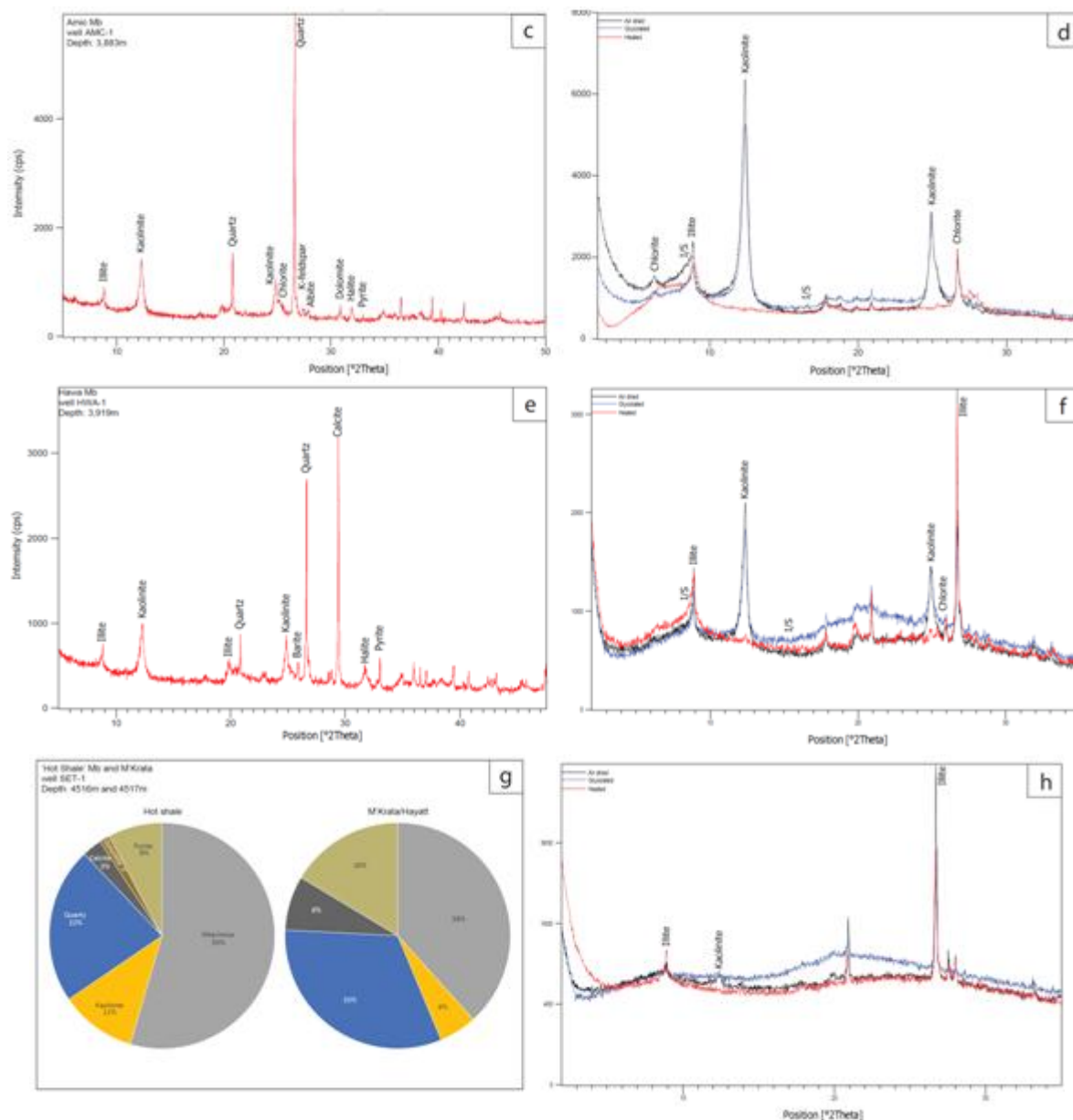


Figure 6: Selected whole rock and clay fraction XRD patterns (diffractograms) generated for the lower Silurian shales of Argiles Principales Formation. Details of members and depth levels are listed in the figure

The Hot shale Member is marked by higher clay content coincident with higher pyrite as well as important quartz amount. Clay fraction is dominated by illite and typical lower kaolinite trend is described from all the studied wells (Fig.4B). It is within this Member that the highest TOC values may occur (Fig.2)

Hawa Member is defined in well HWA-1 in which the succession overlies conformably the hot shale Member. It is generally characterized by high chlorite content in depends of kaolinite with a noted decrease in illite. This increasing trend in chlorite is noted also from wells EPB-1, CEM-1, SET-1 and AMC-1 but with less intensity. This Member is marked by a sudden decrease in pyrite along with quartz. An important increase in clays can be noted in several wells including a positive trend in kaolinite (Figs.4 and 6). This Member is also characterized by a decrease in TOC values in order of magnitude of more than 10% with carbonate are being present in the lower part.

Conversely, Amic Member is marked by a long-term stratigraphically cyclic to static baseline of kaolinite. This characterizes a plateau-like suggesting that the regional clay mineralogy probably recorded at this time span different environmental conditions compared with the previous interval. Illite in this interval remains low with as light positive variations are being noticed for I/S mixed layers.

However, the El Markenti Member is defined in well CEM-1, within which, the highest kaolinite values can be reached along the Argiles Principales. s.

4.3. Carbon isotopic events

Vecoli et al. (2009) presented a detailed $\delta^{13}C_{org}$ acquired along well Tt1 core (Fig.2A), spanning 104.8m around the Jeffara/Argiles Principales formations boundary.

Throughout the early Silurian, $\delta^{13}C_{org}$ values record four shifts reflecting the global paleoceanographic events (Fig.2A).

A close inspection of the carbon isotopic subpeaks demonstrates that, in general, the first maxima was recorded at the Aeronian, being characterized with +2‰ positive shift within the Hot Shale interval. This C_{org} shift is linked to the Sandvika Event of the late Aeronian Carbon Isotopic Event (CIE) (e. g. Jeppsson, 1998; Young et al., 2020). The second excursion, having a higher order of magnitude (+2.5‰), is recorded around the Llandovery/Wenlock boundary which witness the end of Hot Shale Member. This excursion is associated with the Ireviken CIE (e. g. Calner, 2008; McAdams et al., 2017; Young et al., 2020). The aforementioned excursions are coincident with an increase in Gamma ray and TOC (Fig.2). A third shift shyly expressed around the Homerian (+0.9‰ positive shift) is recorded and associated with Mulde Event (e. g. Jaeger 1991; Lenz et al. 2006; Calner, 2008). In addition, towards the Ludfordian, in the Argile Principales s. s. interval, a +3‰ positive shift is recorded. This excursion is likely related to the Lau Event. The interval separating the third and the fourth positive shifts (Mulde and Lau events, respectively) may represent a plateau within the global carbon burial linked to the Silurian global events. The top samples seem not to record the tail end of the Silurian carbon isotopic events as they don't record the return to background values of the global carbon reservoir trend (Fig.2). Similar events were recorded in well E1-NC174 in southwestern Libya (Loydell et al., 2013; Fig.2B)

4.4. Geochemical composition of the early Silurian

A comprehensive geochemical composition has been presented by Soua (2014) and Gambacorta et al. (2016). Figure 8 shows the vertical variations of elemental key ratios and mineralogical composition of the early Silurian Argile Principales Formation in well HYT-1 acquired using SpectroLith logging and Elemental Capture Spectroscopy (ECS) tools.

Ti/Al and Th reflect in general heavy minerals abundance (Morton and Hallsworth, 1994; Armstrong et al., 2005; Pearce et al., 2005; Soua, 2019). Thorium and Ti/Al profiles display a good relationship, while Th and K show a weak trend (Fig.8). This suggests that Th is associated with heavy minerals while K is indicative of clay minerals, mica, and feldspar content (Hurst, 1999; see discussion in Soua, 2014). In another hand, Al and K display somehow similar trends without being strongly matching. They are considered to be controlled by clay minerals. In most cases, Al is associated with kaolinite, whereas K is common in illite and I/S mixed layers (Soua, 2019). In this case, some peaks related to Fe/Al that match those of K and Al could be associated with chlorite. However, the majority of the Fe/Al is generally showing strong relationship with S, which usually reflect the abundance of pyrite. Calcium (Ca/Al) is associated with the carbonate minerals such as calcite, dolomite and probably siderite. However, concentrations of Si in the sandstone and siltstone are generally related to the abundance of quartz and which may indicate variability of grain size. Higher values of Si/Al can be reported to indicate biogenic silica (Soua et al.,

2011; Soua, 2014). The High total gamma ray readings indicative of the early Silurian organic-rich Hot shales sediments is produced exclusively by high presence of uranium (U) coincident with lower concentrations of K and Th in southern Tunisia, which suggest preservation of organic material during reducing environments (Fig.8). The lower part is typically characterized by an increase in S content probably indicative of a settlement of reducing bacterial activity during M'Krata Member (Fig.5). A sudden decrease of Ti/Al is also depicted along the Jeffara/Argiles Principales formations boundary (Fig.8).

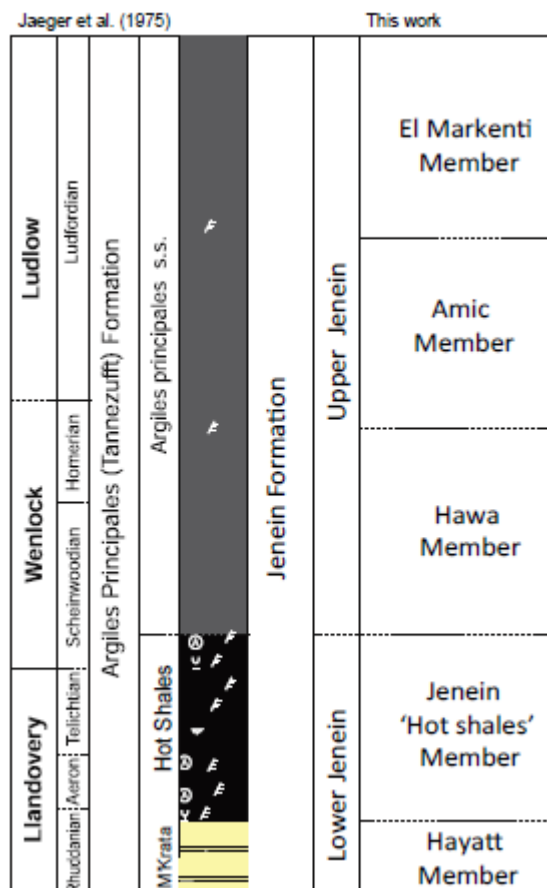


Figure 7: Proposed nomenclature for southern Tunisia in this study and correlation with Jaeger et al. (1975) who defined the Argiles Principales Formation mainly in the Libyan side.

4.5. New lithostratigraphic subdivision

The studied early Silurian Argiles Principales Formation is distributed south of the TTPB structural high within the Berkine and Jeffara Basins, in southern Tunisia. The thickness of the different defined members is given in the Figure 9. The Hot Shale interval can reach 125 m in the southern Tunisian Berkine Basin in more basinal settings whereas it can reach 35 m in the Jeffara Basin.

These Hot shales are considered to be the principal source for the southern Tunisian fields (Luning et al., 2000) labelled laterally Hot shale or Tannezufft Formation by most of the petroleum geologists. In the Southern Tunisian Berkine and Jeffara basins, its presence is certainly important to cover one of the needed petroleum system, but the name chosen is not reliable since the huge distance separating the type

section (Oued Tannezzouft, located in Ghat area in Libya; Desio, 1936; Klitzsch, 1969; Collomb, 1962) with the studied sequences (see Fig 2B).

In this contribution, it is proposed to limit the term ‘‘Hot Shale/Argiles Principales/Tannezuft Formation’’ for the Libyan side and suggest ‘‘Jenein Formation’’ inferred from Jenein field in southern Tunisia, where the early Silurian is geochemically best studied.

The Hot Shale Member is replaced herein by the term ‘‘Jenein Hot shales’’ Member and M’Krata, which terminology belongs to Algeria is replaced by Hayatt Member inferred from well HYT-1 (Fig.7). The Hayatt and Jenein Hot shales members would pertain to Lower Jenein Formation. However, the defined Hawa, Amic and El Markenti members belong to the Upper Jenein Formation (see Fig.7 for more explanation). Figure 9 shows thickness maps respective to the defined members in Jenein Formation (=Argiles Principales) acquired using interpolation of available well data points (calculated thickness of each member). These maps were generated to help understand the paleodeposition model of the Jenein Formation (each subdivided member) throughout the generalized periglacial setting after the ice-sheet retreat. This may imply the paleofloor geometry or induce one or more tectonic phases that modelled the general distribution of different facies composing the Jenein Formation

5. Discussion

5.1. General paleoenvironmental changes

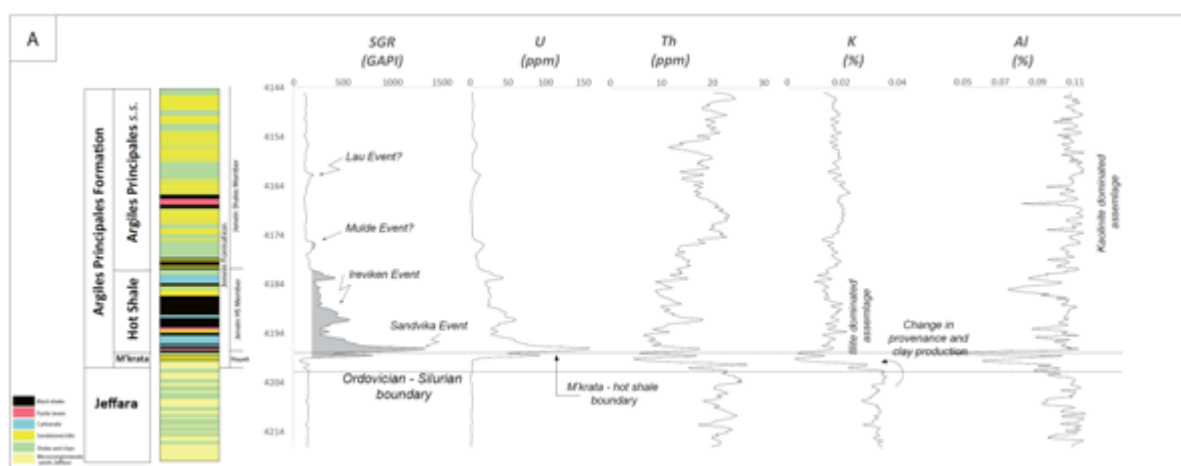
5.1.1. Geochemical variation

Along the lower Jenein (=lower Argiles Principales) Formation, the Si/Al ratio vertical variation is not correlative with clastic proxies peaks including Al, K and in some circumstances Ti/Al (as it is chiefly considered to be related to heavy minerals and reflecting changes in provenance). In

these levels, the silica is not clearly associated with clay-bearing minerals nor quartz. In this case, it may probably originate from biogenic precursor material rather than from detrital quartz. Comparison of elevated silica values in Hayatt (=M’Krata) Member, in well HYT-1 (Fig.8) with the average shale values (e. g. Brumsack, 2006; Tribouvillard et al., 2006; Soua et al., 2011), probably implies the existence of a local elevated productivity of biogenic silica-secreting organisms (Soua, 2014). However, towards the top, the silica is associated with the detrital proxies and may originate from detrital quartz instead. Many studies conducted on black shales had documented a biogenic origin of quartz content from silica-bearing microorganisms (Chalmers et al., 2012; Turgeon and Brumsack, 2006; Soua et al., 2011).

In general, Th and Ti are related to source area changes (Soua, 2019). Both elements can be associated with a large variety of ultrastable heavy mineral suites, which are rarely affected by alteration (Pettijohn et al., 1987; Morton and Hallsworth, 1994; Armstrong et al., 2005; Pearce et al., 2005; Soua, 2016). In addition, the elements Th and Ti can be found in the clay, silt, and sand sized material as they are concentrated in the very fine fraction of the rock. Figure 8 shows a severe change in provenance during the transition between Jeffara and Hayatt Member. This change is accommodated by a shift to a different source area of sedimentation during the retreat of the regional glacial ice-sheet of the end of Ordovician. This may probably have been caused by the global sea level rise. The sharp negative change of Ti/Al is taken in this study to reflect the Jeffara/Hayatt boundary and therefore the transition from Ordovician to Silurian (Fig.8).

The early Silurian is also marked by a peak of Ca/Al, which characterizes concentration of carbonate minerals including calcite, dolomite and siderite. The highest peak is located in the top of Hayatt Member and marks the onset of the Hot Shale interval. The other Ca/Al peaks seem not to be correlative with pyrite profile and organic material.



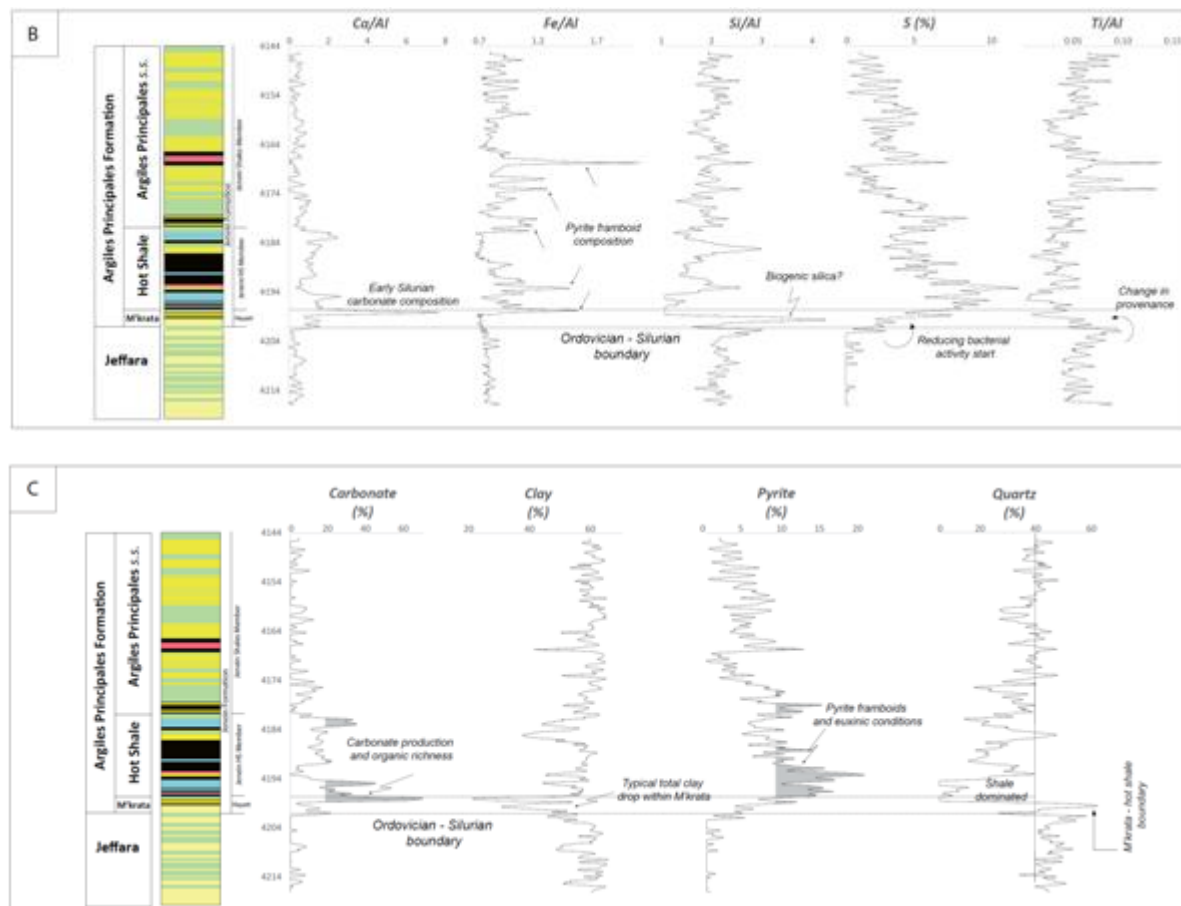


Figure 8. Wireline, SpectroLith logging and Elemental Capture Spectroscopy (ECS) for the early Silurian Hot shale interval and overlying shales of the Argiles Principales Formation in well HYT-1. **A.** SGR (GAPI), U (ppm), Th (ppm), K (%) and Al (%). The SGR is interpreted in terms of the Silurian biotic events along with the Ordovician-Silurian boundary as well as M'Kratá-hot shale transition limit. **B.** Ca/Al, Fe/Al, Si/Al, S (%) and Ti/Al. data acquired is interpreted in terms of carbonate composition along with pyrite framboid presence, biogenic silica, reducing bacterial activity/microbial mats and changes in provenance indication (see text for more details). **C.** Carbonate, clay, pyrite and quartz content. Data acquired is interpreted in terms of carbonate production, organic richness, clay content, pyrite framboids/euxinic conditions and quartz/clay dominance.

5.1.2. Mineralogical composition

The whole rock mineralogy of the Jenein Formation (=Argiles Principales) is dominated by quartz, accounting for 20%-35% in Hayatt and Jenein Hot Shale members along with 30% to 50% in the upper Jenein Formation, and kaolinite producing 5%-10% in lower Jenein to reach more than 40% in upper Jenein formation. Illite is considered as one of the major minerals along the Hot shale Member with pyrite being a major mineral in the lowermost part of the formation (Fig.4).

Preceding studies (Jaeger et al., 1975; Bellini and Massa, 1980; Klitzsch, 1981) propose that the Jenein (=Argiles Principale/ Tanezzuft) shale may have been deposited in a marine setting with alternations of silty to sandy levels with hummocky cross stratifications (HCS). In fact, close inspection of the Silurian cores and cuttings taken in southern Tunisia (Soua, 2009), shows that the shales overlying the Hot shale Member are made of very fine shaly grained material concentrated within muddy levels along with tidal currents along with storm waves with tidal inlets are being affecting the siltstone and sandstone levels (Soua, 2009).

The Hot Shale interval is characterized by dark mudstone with remarkably high gamma ray values and high TOC amount. Bioturbation and graptolites are frequently present along the dark shales (Fig.5). This infers a decantation in anoxic environments along with a preservation of type II organic matter (Rezouga et al., 2012) in an offshore setting.

A minor percentage of the quartz content is accounted during the onset of the Hot shale Member which record a slight increase in carbonate and elevated pyrite contribution along with clays (Figs.4 and 8). Although the general quartz content of the lower part of the Jenein Hot Shale Member is quietly low, the related subpeaks seem to correlate with those of pyrites and TOC content (wells HYT-1 and SET-1, Figs.4 and 8). The abundance of illite along the Hot Shale interval is explained by the fact that this mineral is formed due to smectite alteration during burial. It is worthy to note that no discrete smectite crystallographic plane is present (Fig.6). According to Ghandour et al. (2003), the dominating presence of illite is probably indicative of a cold and dry paleoclimate. This is in accordance with the global and regional early Silurian paleoclimate that reigned during the deposition of Hot Shale Member.

The clay fraction XRD results show that clay minerals identified along the Hot shale interval are dominated by illite (Fig.4). Mixed layers illite/smectite (I/S, R1; Fig.6),

kaolinite, and chlorite are reported low to absent in this interval but vary intensely in the overlying members.

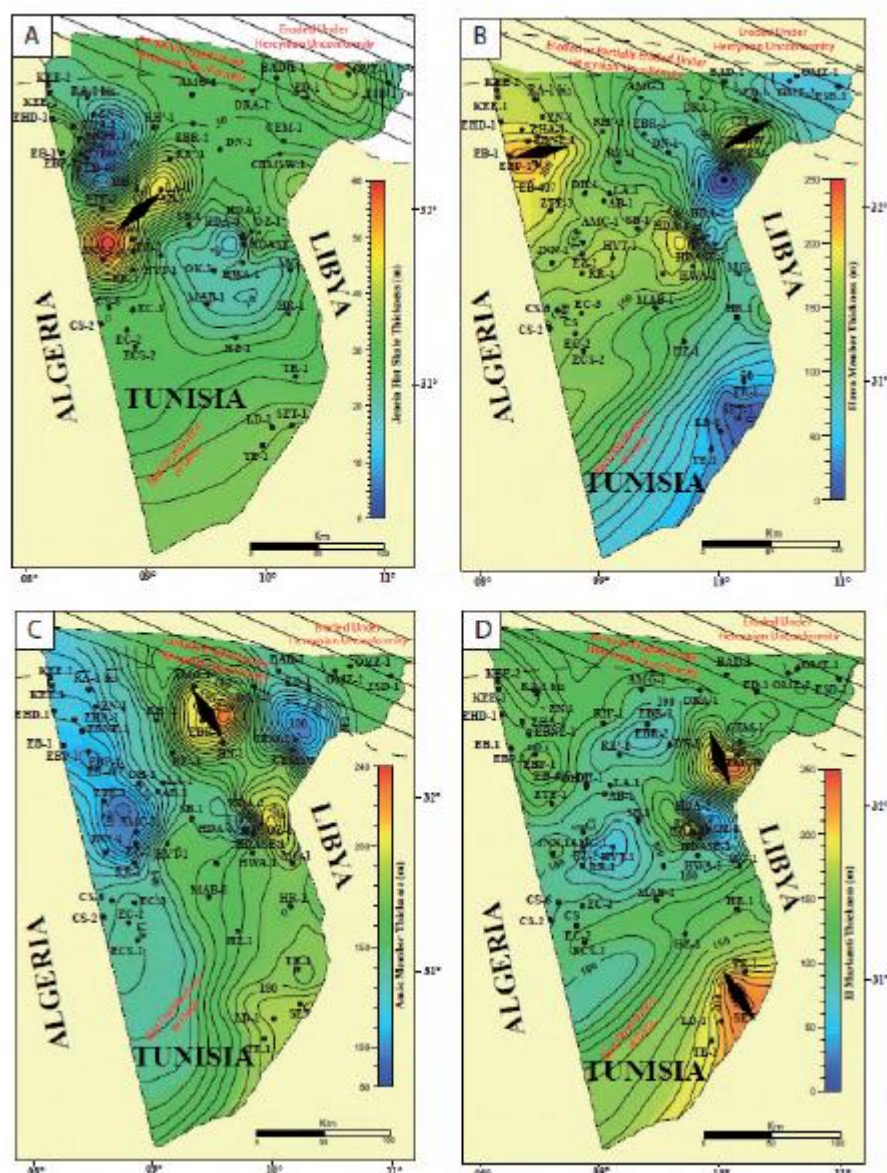


Figure 9: Generated thickness maps for the early Silurian Jenein Formation (=Argiles Principales Formation) members in Southern Tunisia. **A.** thickness map of hot shales (including M'krata member if it exists). **B.** Thickness map of Hawa Member. **C.** Thickness map of Amic Member. **D.** Thickness map of El Markenti Member.

The variation of clay mineral assemblages along Jenein Formation may be indicative of changes in paleoenvironment and paleoclimate (McLennan et al., 1993; Deconinck et al., 2000; Meng et al., 2012). For example, according to some authors (e. g. Lan, 1990; Tang et al., 2002; Worden and Morad, 2003), the mineral kaolinite can originate in humid and warm conditions by intense feldspars decomposition under strong leaching conditions such as important drainage and acid rainfall. However, this assumption is in contrast with the early Silurian periglacial paleoclimate conditions during which the Jenein Formation has been deposited (Gambacorta et al., 2016).

Hassan and Massa (1975) presented interesting geochemical and mineralogical study on what they called "radioactive zone" (high radioactive gamma ray interval or 'hot shale').

The high percentages of organic material and important concentrations of trace elements were attributed to shallow and calm anaerobic environment resulting from a reducing bacterial activity, which in turn may have caused the precipitation of the carbonates. They identified the predominance of the kaolinite along the upper part of the formation on top of the radioactive zone and interpreted the ensemble to be marked by essential acid conditions capable of generating processes of neoformation or at least of preserving this mineral. Intense feldspars decomposition under strong acid rainfall or water drainage can be responsible to form kaolinite in the upper Jenein Formation. The reason why, we adopt the assumption presented by Hassan and Massa (1975) as a paleoenvironmental variation rather than a categorical paleoclimatic change.

Chlorite can form due to silicates leaching either from smectite transformation or enrichment by Mg cation due to physical weathering (Ehrmann et al., 1992). However, provenance and diagenesis conditions should be taken into consideration to satisfy a reliable and plausible clay mineralogical interpretation.

The whole rock XRD results of wells EBP-1, CEM-1, AMC-1, HWA-1 and SET-1 show that feldspars including plagioclase (albite) and k-feldspar (microcline) are relatively low to absent in the intervals enriched in kaolinite. The absence of feldspars within these levels may involve intense weathering.

In the Hawa Member, the shales are composed of wavy to lenticular bedding interlayered with heterolithic sandstones with ripple marks and abundant bioturbations. These sedimentological features are indicative of wave action (e. g. De Raaf et al., 1977). Plagioclase in this interval record relatively high value (Fig.4A) coincident with lower quartz and higher clay amounts. The XRD clay fraction analysis shows a slight increase in I/S mixed layers and an important elevation in kaolinite.

The overlying Amic Member, heterolithic sandstone deposits persist with alternation of HCS sandstone / mud. In the upper part of the member well sorted along fine to medium grained sandstone beds marked with stacked HCS are rarely present. This deposition environment is diagnostic of storm domination as part of a shoreface setting. This member is highly enriched in kaolinite, while chlorite records high values in wells SET-1 and HWA-1 reaching ca.5%.

The El Markenti Member is marked by a clean well sorted fine to medium grained with low angle to horizontal plane parallel bedding (Soua, 2009).

As conclusive remarks for this section, in the lowermost part of the Jenein Formation, quartz amount increases with the TOC/pyrite content (Figs.4 and 8), indicating a probable important biogenic source is responsible for the quartz peak in the top of Hayatt Member. However, the overlying levels no obvious relationship is present between quartz and TOC amount (Figs.4 and 8). This may imply a change in source area or implementation of a new provenance. The clay content in Hayatt Member is between 20 and 30% in average; while in Jenein Hot Shale is set to be around 45%. In the upper Jenein Formation the clay can reach 60%. Figures 4 and 8 show a negative relationship between clay amount and TOC. This can be explained by the fact that organic matter enrichment is controlled by the terrestrial flux.

5.1.3. Classification of the mineral composition

Shale reservoir mineral composition is broadly variable and changes according to several paleoenvironmental factors. Figure 10A shows a ternary diagram created using data generated from total clay (Illite, kaolinite and chlorite), total carbonate (calcite, dolomite and siderite) and quartz being modified from Passey et al. (2010). These authors highlighted mineral field composition of Eagleford, Barnett and clay-rich gas-bearing mudstone, where mineral groups vary entirely according to the environment of deposition and play composition. Samples from well SET-1 have been plot to this diagram showing that Hot shale mineral composition tend to lie Barnett and Clay-rich gas bearing mudrock field of data with one single sample is being carbonate-rich. Figure 10B shows ternary classification plot that is built on established relationships between normalized proportions of quartz feldspar-mica (WQFM), total clay (WCLA) and total carbonate (WCAR) (Gamero-Diaz et al., 2013).

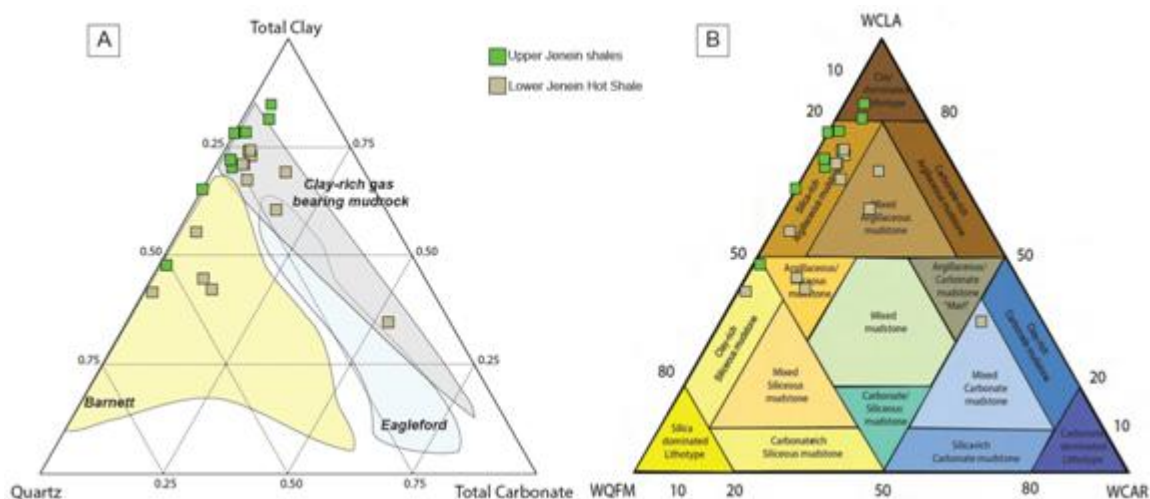


Figure 10: Ternary diagrams (quartz–clay–carbonate) of well SET-1. **A.** data distribution along Barnett, Eagleford and clay-rich gas bearing mudrock of lower and upper Jenein formation. (modified from Passey et al., 2010). **B.** data composition of the aforementioned samples (modified from Gamero-Diaz et al., 2013)

5.2. Some remarks on the Silurian biotic events in Southern Tunisia

Several biological and geochemical events coupled to global carbon excursions during the Silurian were identified and described (e. g., Munnecke et al., 2003; Calner, 2008;

Cramer et al., 2011; Melchin et al., 2020; Biebesheimer et al., 2021).

5.2.1. Carbon isotopic excursions (CIEs)

Vecoli et al. (2009) presented the only $\delta^{13}\text{C}_{\text{org}}$ measured for the early Silurian in southern Tunisia in well Tt-1 identified

for the first time in Gondwanan high-latitude settings (North Africa). These values are very comparable to what have been presented later by Loydell et al. (2013) in well E1-NC174 in south-western Libya (Fig.2B). In southern Tunisia, organic carbon isotopic values range between -30.79‰ and -27.42‰. Four (04) major positive carbon isotope excursions (CIEs) can be depicted (see Figure 2A) and could be assigned to the global Silurian bioevents.

The two first reported CIEs (Fig.2A) are associated with the late Aeronian and Telychian-Sheinwoodian (Llandovery-Wenlock boundary) biotic events (e. g. Cramer and Saltzman, 2005; Kaljo and Martma, 2006; Calner, 2008; Bancroft et al., 2015; McAdams et al., 2017; Young et al., 2020). The late Aeronian event is commonly documenting an important extinction event including many taxa from the early Silurian well known to be the Sandvika Event (e. g. Jeppsson, 1998; Young et al., 2020). In fact, substantial extinction/turnover in graptolite assemblages during that time has been reported in the Baltic Basin, especially along *Sedgwickii* graptolite biozones (Zone 21) (Storch, 1995; Melchinet al., 1998; Crompton et al., 2016). Other authors reported major turnover associated with acritarchs and other marine taxa (e. g. Jeppsson, 1998). In southern Tunisia and eastern Libya, the related carbon isotopic signatures are present, indicating that the Silurian events covered at least some parts of North African Gondwanan high latitudes (Fig.2).

5.2.2. Early Silurian global events

In well Tt-1 the late Aeronian CIE, associated with the Sandvika Event, appears to be coincident with *Sedgwickii* biozone described by Bonnefous (1963) and Jaeger et al. (1975) (Fig.2). The latter CIE is also associated with *S. maennili* and *C. edjelensis* chitinozoans assemblages described by Vecoli et al. (2009). The second CIE is likely recording the Ireviken global bioevent (e. g. Jeppsson, 1987; Saltzman 2001; Kaljo et al.2004; Noble et al.2005; Brand et al.2006; Calner, 2008; Lehnert et al., 2010; Cramer et al., 2012; McAdams et al., 2019; Melchin et al., 2020; Hartke et al., 2021) known as the Silurian major marine extinction bioevent (Calner, 2008). The Figure 2 shows that the Ireviken Event is spanning the late Llandovery-early Wenlock interval boundary. The isotopic data imply that both the Sandvika and Ireviken bioevents occurred in high-latitude settings (e. g. Tunisia and Libya; Fig.2). According to Calner (2008), the start of the event is depicted by the chitinozoan biostratigraphic zone *Margachitinamargaritana* which occurred entirely during a regressive sequence (Loydell et al., 2003; 2013).

In southern Tunisia, the *lundgreni* graptolite zone records a third CIE peak (Fig.2) that is coincident most likely with the Mulde Event (e. g. Kaljo et al.1997; Cramer et al.2006; Cramer et al., 2012; Cooper et al., 2014; Crompton et al., 2016). The event is associated with a severe faunal turnover during the Lower Homerian, during which a graptolites mass extinction is reported within a generalized anoxic event and known under *lundgreni* Event name (Koren' 1991; Jaeger 1991; Lenz et al.2006; Cramer et al.2006; Calner, 2008; Cramer et al., 2012; Cooper et al., 2014; Sullivan et al., 2016; Danielsen et al., 2019). In the top of well Tt-1 Silurian sequence, the most remarkable CIE of the entire section

being represented by a larger magnitude than the Sandvika, Ireviken and Mulde events (Fig.2). This CIE is linked in this study to the Lau Event (e. g. Andrew et al.1994; Kaljo et al.1997; Saltzman 2001; Munnecke et al., 2003; Lehnert et al.2007; Calner, 2008; Saltzman and Thomas, 2012; Bowman et al., 2019). According to Calner (2008), it is quite difficult to explain the Lau vast magnitude that illustrates the most spectacular positive carbon isotopic excursion of the whole Phanerozoic.

Figure 2B is an attempt to correlate the aforementioned Silurian bioevents between Tunisia and Libya. Using the available data (Loydell et al., 2013), it was possible to identify the extinction events in well E1-NC174 (see Figure 2 for location).

The only interesting difference that can be deduced from the Libyan paleoceanographic reconstruction is that the $\delta^{13}\text{C}_{\text{org}}$ peaks and subpeaks related to the Ireviken and Lau events, are not correlatable with the TOC maxima, although other elevated isotopic values are associated with high TOC. This may imply on stratigraphic significance of the regional Silurian excursions. In the Libyan side, after the onset of $\delta^{13}\text{C}_{\text{org}}$ excursions associated with the Ireviken event (Llandovery/Wenlock boundary) and most probably the Lau event during the Ludfordian, the elevated TOC seem to have generally undergone important variation. In southern Tunisia, only the Mulde Event (lower Homerian) is associated with low TOC and related CIE subpeaks do not correlate with elevated organic carbon (Fig.2).

6. Conclusion

Whole rock and clay fraction data of the Jenein (=Argiles Principales) Formation from southern Tunisia Berkine Basin (northern Gondwana) provide new insight on the deposition of the early Silurian 'Hot' Shale' and overlying succession.

Comparison with the overlying upper Jenein shales, the organic-rich Hot Shale interval required specific conditions to produce higher amount of illite in depends of other clay minerals. These conditions were obviously more prevalent in the early Silurian (Hayatt and Hot Shale members) than later in the overlying succession. The transition from the organic-rich black shales into mudrocks and shales of the Hawa Member records enhanced preservation of widespread enrichment of kaolinite, which marks the overlying member as well. Minimal variability is mostly noted within chlorite and illite-smectite mixed layers (I/S) in the studied section.

The very low content to absence of feldspar (mainly k feldspar/microcline) may be indicative of intense feldspars decomposition under strong acid water drainage, which can be responsible to form kaolinite in the upper Jenein Formation. The predominance of the kaolinite on top of the 'Hot shale' Member marks essential acid conditions capable of generating processes of neof ormation or preservation.

The small-sized pyrite framboids described from the early Silurian 'Hot Shale' Member coincident with very high pyrite concentration are indicative of euxinic conditions. These severe paleoenvironmental circumstances coincident with high percentages of organic material along with

important concentrations of primary productivity and redox proxies may indicate shallow and calm anaerobic environment resulting from activity of sulfate-reducing bacteria, causing most probably the precipitation of the few carbonates beds in the early Silurian.

This succession related to Jenein Formation has been linked to intensified oxygen minimum zone (OMZ) expansion along the Gondwana margins during global to regional anoxic mass-extinction events (Sandvika, Ireviken, Mulde and Lau), which were controlled by multiple phases and factors including ice-sheet melting, tectonics, paleoceanography, etc.

The described isotopic organic carbon excursions are most notably associated with widespread bottom water anoxia, which have triggered organic carbon preservation during subsequent burial.

Acknowledgement

I would like to thank Pr. David Lloydell and Pr. Omer Bozkaya for reviewing an earlier draft of the manuscript. ETAP is also thanked for providing the wireline data used in this paper.

References

- [1] Abuhmida, F., 2013. Palynological Analysis of the Ordovician to Lower Silurian Sediments from the Murzuq Basin, Southwest Libya, unpublished PhD, 641p.
- [2] Andrew AS, Hamilton PJ, Mawson R, Talent JA, Whitford DJ (1994) Isotopic correlation tools in the Middle Palaeozoic and their relation to extinction event. *APEA Journal* 34: 268-277
- [3] Armstrong HA, Turner BR, Makhlof IA, Williams M, Al Smadi A, Abu Salah A (2005). Origin sequence stratigraphy and depositional environment of an Upper Ordovician Hirnantian) peri-glacial black shale, Jordan: *Palaeogeography, Palaeoclimatology, Palaeoecology* 220: 273-289.
- [4] Bancroft, A. M., Brunton, F. R., Kleffner, M. A., 2015. Silurian conodont biostratigraphy and carbon ($\delta^{13}\text{C}_{\text{carb}}$) isotope stratigraphy of the Victor Mine (V-03-270-AH) core in the Moose River Basin. *Canadian Journal of Earth Sciences*, 52 (12), 1169-1181.
- [5] Bellini, E., Massa, D., Salem, M. J.1980. A stratigraphic contribution to the Palaeozoic of the southern basins of Libya. *The geology of Libya*, 1, 3-56.
- [6] Ben Ferjani, A., Burollet, P., Mejri, F., 1990. *Petroleum Geology of Tunisia*, ETAP, 193p.
- [7] Beuf, S., Biju-Duval, B., De Charpal, O., Rognon, P., Gariel, O., Bennacef, A., 1971. Les grès du Paléozoïque inférieur au Sahara. *Sci. Technol. Pet* 18, 464p.
- [8] Biebesheimer, E. J., Cramer, B. D., Calner, M., Barnett, B. A., Oborny, S. C., & Bancroft, A. M.2021. Asynchronous $\delta^{13}\text{C}_{\text{carb}}$ and $\delta^{13}\text{C}_{\text{org}}$ records during the onset of the Mulde (Silurian) positive carbon isotope excursion from the Altajme core, Gotland, Sweden. *Chemical geology*, 576, 120256.
- [9] Bonnefous, J., 1963. Synthèse stratigraphique sur le Gothlandien des sondages du Sud Tunisien. *Rev. Inst. Fr. Pétr.* XVIII 10, 123–133.
- [10] Boote, D. R. D., Clark-Lowes, D. D., Traut, M. W., 1998. Palaeozoic petroleum systems of North Africa. In: Macgregor, D. S., Moody, R. T. J., Clark-Lowes, D. D. (Eds.), *Petroleum Geology of North Africa*. Geological Society (London) Special Publication 132, pp.7–68.
- [11] Bowman, C. N., Young, S. A., Kaljo, D., Eriksson, M. E., Them, T. R., Hints, O., Martma, T., Owens, J. D.2019. Linking the progressive expansion of reducing conditions to a stepwise mass extinction event in the late Silurian oceans. *Geology*, 47 (10), 968-972.
- [12] Brand U, Azmy K, Veizer J (2006) Evaluation of the Salinic I tectonic, Cancañari glacial and Ireviken biotic events: biochemostratigraphy of the Lower Silurian succession in the Niagara Gorge area, Canada and USA. *Palaeogeography, Palaeoclimatology, Palaeoecology* 241: 192-213
- [13] Brumsack, H. J., 2006. The trace metal content of recent organic carbon-rich sediments: implications for Cretaceous black shale formation. *Palaeogeogr. Palaeoclimatol. Palaeoecol.*232 (2), 344–361.
- [14] Butcher, A., 2013. Chitinozoans from the middle Rhuddanian (lower Llandovery, Silurian) ‘hot’ shale in the E1-NC174 core, Murzuq Basin, SW Libya. *Rev. Palaeobot. Palynol.*198, 62–91.
- [15] Calner, M., 2008, Silurian global events-At the tipping point of climate change, in Elewa, A. M. T., ed., *Mass Extinctions*: Berlin, Springer-Verlag, p.21–57.
- [16] Carr, I. D., 2002. Second-order sequence stratigraphy of the Palaeozoic of North Africa. *J. Pet. Geol* 25 (3), 259–280.
- [17] Chalmers, G. R. L., Ross, D. J. K., Bustin, R. M., 2012. Geological controls on matrix permeability of devonian gas shales in the Horn river and liard basins, northeastern British Columbia, Canada. *Int. J. Coal Geol.*103, 120–131.
- [18] Cluff, B., Miller, M., 2010. Log evaluation of gas shales: a 35-year perspective. In: *The Denver Well Logging Society. SPWLA 52th Annum Logging Symposium. DWLS Luncheon*, Denver.
- [19] Cocks, L. R. M., Torsvik, T. H., 2002. Earth geography from 500 to 400 million years ago: a faunal and palaeomagnetic review. *J. Geol. Soc.*159 (6), 631–644.
- [20] Collomb, G. R., 1962. Etude géologique du Jebel Fezzan et de sa bordurepaleozoïque. *Compagnie Française des Pétroles, Notes et Mémoires* I, 26 S., Paris.
- [21] Cooper, R. A., Sadler, P. M., Munnecke, A., Crampton, J. S., 2014. Graptoloid evolutionary rates track Ordovician–Silurian global climate change. *Geological Magazine*, 151 (2), 349-364.
- [22] Craig, J., Rizzi, C., Said, F., Thusu, B., Luning, S., Asbali, A. I., Hamblett, C., 2008. Structural styles and prospectivity in the Precambrian and Palaeozoic hydrocarbon systems of North Africa. *Geol. East Libya* 4, 51–122.

- [23] Cramer, B. D., Saltzman, M. R., 2005. Sequestration of ^{12}C in the deep ocean during the early Wenlock (Silurian) positive carbon isotope excursion. *Palaeogeogr. Palaeoclimatol. Palaeoecol.* 219 (3), 333–349.
- [24] Cramer, B. D., Kleffner, M. A., Saltzman, M. R., 2006. The late Wenlock Mulde positive carbon isotope ($\square^{13}\text{C}_{\text{carb}}$) excursion in North America. *GFF* 128 (2), 85–90.
- [25] Cramer, B. D., Brett, C. E., Melchin, M. J., Männik, P., Kleffner, M. A., McLaughlin, P. I., Loydell, D. K., Munnecke, A., Jeppsson, L., Corradini, C., Brunton F., Saltzman, M. R., 2011. Revised correlation of Silurian Provincial Series of North America with global and regional chronostratigraphic units and $\square^{13}\text{C}_{\text{carb}}$ chemostratigraphy. *Lethaia*, 44 (2), 185–202.
- [26] Cramer, B. D., Condon, D. J., Söderlund, U., Marshall, C., Worton, G. J., Thomas, A. T., Calner, M., Ray, D. C., Perrier, V., Boomer, I., Patchett, P. J., Jeppsson, L., 2012. U-Pb (zircon) age constraints on the timing and duration of Wenlock (Silurian) paleocommunity collapse and recovery during the “Big Crisis”. *Bulletin*, 124 (11-12), 1841–1857.
- [27] Crampton, J. S., Cooper, R. A., Sadler, P. M., and Foote, M., 2016. Greenhouse-icehouse transition in the Late Ordovician marks a step change in extinction regime in the marine plankton: Proceedings of the National Academy of Sciences of the United States of America, v.113, p.1498–1503
- [28] Daniels, R. P., Emme, J. J., 1995. Petroleum system model, eastern Algeria, from source rock to accumulation: when, where and how. In Proceedings of the Seminar on Source Rocks and Hydrocarbon Habitat in Tunisia, pp.101–124.
- [29] Danielsen, E. M., Cramer, B. D., Kleffner, M. A., 2019. Identification of a global sequence boundary within the upper Homerian (Silurian) Mulde Event: High-resolution chronostratigraphic correlation of the midcontinent United States with Sweden and the United Kingdom. *Geosphere*, 15 (3), 839–855.
- [30] Davidson, L., Beswetherick, S., Craig, J., Eales, M., Fisher, A., Himmali, A., Smart, J., 2000. The Structure, Stratigraphy and Petroleum Geology of the Murzuq Basin, Southwest Libya. Geological Exploration of the Murzuq Basin. Elsevier, Amsterdam, pp.295–320.
- [31] De Raaf, J. F. M., Boersma, J. R., Van Gelder, S., 1977. Wave-generated structures and sequences from a shallow marine succession, Lower Carboniferous, County Cork, Ireland. *Sedimentology*, 24 (4), 451–483.
- [32] Deconinck, J. F., Blanc-Valleron, M. M., Rouchy, J. M., Camoin, G., Badaut-Trauth, D., 2000. Palaeoenvironmental and diagenetic control of the mineralogy of upper cretaceous-lower tertiary deposits of the central Palaeo-Andean basin of Bolivia (Potosi area). *Sediment. Geol.* 132, 263–278.
- [33] Desio, A., 1936. Riassuntosullapresenza del Siluricofossiliferonel Fezzan. *Boll. Soc. Geol. Ital.* 55, 319–356.
- [34] Dickinson, W. R., Beard, L. S., Brakenridge, G. R., Erjavec, J. L., Ferguson, R. C., Inman, K. F., Knepp, R. A., Lindberg, F. A., Ryberg, P. T., 1983. Provenance of North American Phanerozoic sandstones in relation to tectonic setting. *Geological Society of America Bulletin*, 94 (2), 222–235.
- [35] Dummond, M., Rasul, S. M., 1985. Well Cherguia-1, Palynological Final Report, Selected Samples (Interval 2, 108.2m-2, 292m), Project Number 1420 Paleoservices, AMOCO Internal Report, 21p.
- [36] Ehrmann, W. U., Melles, M., Kuhn, G., Grobe, H., 1992. Significance of clay mineral assemblages in the Antarctic Ocean. *Mar. Geol.* 107, 249–273.
- [37] Fabre, J., 1988. Les séries paléozoïques d’Afrique: une approche. *J. Afr. Earth Sci. (and the Middle East)* 7 (1), 1–40.
- [38] Gambacorta, G., Caronni, V., Antonielli, E., Massara, E. P., Riva, A., Scotti, P., Trincianti, E., Erba, E., 2016. Hot shale in an ice world: Paleoceanographic evolution of the northern Gondwana margin during the early Paleozoic (Tanezzuff Formation, Tunisia). *Marine and Petroleum Geology*, 72, 393–411.
- [39] Gamero-Diaz, H., Miller, C., Lewis, R., 2013. sCore: a mineralogy based classification scheme for organic mudstones. In SPE Annual Technical Conference and Exhibition. SPE-166284-MS, SPE Annual Technical Conference and Exhibition September, 2013, New Orleans, Louisiana, USA, OnePetro.
- [40] Ghandour, I. M., Masuda, H., Maejima, W., 2003. Mineralogical and chemical characteristics of Bajocian-Bathonian shales, G. Al-Maghara, North Sinai, Egypt: climatic and environmental significance. *Geochem. J.* 37, 87–108.
- [41] Ghienne, J. F., Deynoux, M., 1998. Large-scale channel fill structures in Late Ordovician glacial deposits in Mauritania, western Sahara. *Sed. Geol.* 119 (1), 141–159.
- [42] Ghienne, J. F., Boumendjel, K., Paris, F., Videt, B., Racheboeuf, P., Salem, H. A., 2007. The Cambrian–Ordovician succession in the Ougarta Range (western Algeria, North Africa) and interference of the Late Ordovician glaciation on the development of the Lower Palaeozoic transgression on northern Gondwana. *Bull. Geosci.* 82 (3), 183–214.
- [43] Grunsky, E. C., Drew, L. J., Woodruff, L. G., Friske, P. W. B., Sutphin, D. M., 2013. Statistical variability of the geochemistry and mineralogy of soils in the Maritime Provinces of Canada and part of the Northeast United States: 249–266.
- [44] Guiraud, R., Bosworth, W., Thierry, J., Delplanque, A., 2005. Phanerozoic geological evolution of Northern and Central Africa: an overview. *J. Afr. Earth Sci.* 43 (1), 83–143.
- [45] Hallett, D., 2002. *Petroleum Geology of Libya*. Elsevier, p.509.
- [46] Hartke, E. R., Cramer, B. D., Calner, M., Melchin, M. J., Barnett, B. A., Oborny, S. C., Bancroft, A. M., 2021. Decoupling $\square^{13}\text{C}_{\text{carb}}$ and $\square^{13}\text{C}_{\text{org}}$ at the onset of the Ireviken Carbon Isotope Excursion: $\Delta^{13}\text{C}$ and organic carbon burial (forg) during a Silurian oceanic anoxic event. *Global and planetary change*, vol.196, p.103373.
- [47] Hassan, M., Massa, D., 1975. Some geochemical and sedimentological aspects of the Lower Silurian of North Africa. *Congr. Int. Sédiment., Nice, Extr. Publ.: Congrès*, v.1, p.97–102.

- [48] Hurst, A., 1999. Textural and geochemical micro-analysis in the interpretation of clay mineral characteristics; lessons from sandstone hydrocarbon reservoirs. *Clay Miner.*34 (1), 137–149.
- [49] Jaeger H., 1991. New standard graptolite zonal sequence after the "big crisis" at the Wenlockian/Ludlovian boundary (Silurian). *Neues Jahrbuch für Geologie und Paläontologie, Abhandlungen* 182: 303-354.
- [50] Jaeger, H., Bonnefous, J., Massa, D., 1975. Le silurien en Tunisie, ses relations avec le silurien de Lybie nord-occidentale. *Bull. Soc. Géol. Fr.*17, 68–76.
- [51] Jeppsson, L., 1987. Lithological and conodont distributional evidence for episodes of anomalous oceanic conditions during the Silurian. In: Aldridge, R. J. (ed.) *Palaeobiology of conodonts*. Ellis Horwood, Chichester, West Sussex, 129-145
- [52] Jeppsson, L., 1998, Silurian oceanic events: Summary of general characteristics, in Landing, E., and Johnson, M. E., (Eds), *Silurian Cycles: Linkages of Dynamic Stratigraphy with Atmospheric, Oceanic, and Tectonic Changes: James Hall Centennial Volume: Albany, New York, New York State Museum Bulletin 491*, p.239–257.
- [53] Kaljo D, Martma T., 2006. Application of carbon isotope stratigraphy to dating Baltic Silurian rocks. *GFF* 128: 161-168
- [54] Kaljo, D., Kipli, T., Martma, T., 1997. Carbon isotope event markers through the Wenlock–Pridoli sequence at Ohesaare (Estonia) and Priekule (Latvia). *Palaeogeogr. Palaeoclimatol. Palaeoecol.*132 (1), 211–223.
- [55] Kaljo D, Martma T, Neuman BEE, Rønning K 2004. Carbon isotope dating of several uppermost Ordovician and Silurian sections in the Oslo region, Norway. *Wogogob meeting abstract* 51-52.
- [56] Klitzsch, E., 1969. Stratigraphic section from the type areas of Silurian and Devonian strata at western Murzuk Basin (Libya). In: Kanes, W. H. (Ed.), *Geology, Archaeology and Prehistory of the Southwestern Fezzan, Libya*. Petroleum Exploration Society of Libya, Eleventh Annual Field Conference, pp.83–90.;
- [57] Klitzsch, E., 1981. Lower Palaeozoic Rocks of Libya, Egypt and Sudan. In: Holland C. H. (ed.), *Lower Palaeozoic of the Middle East, Eastern and Southern Africa and Antarctica*, New York, pp.131-163; Wiley, London.
- [58] Koren´ T. N.1991. The *lundgreni* extinction event in central Asia and its bearing on graptolite biochronology within the Homeric. *Proceedings of the Estonian Academy of Sciences, Geology* 40: 74-8.
- [59] Lan, X.-H., 1990. Clay minerals as an index of paleoclimate. *Geol. Sci. Technol. Inf.*9, 31–35;
- [60] Le Heron, D. P., Craig, J., 2008. First-order reconstructions of a Late Ordovician Saharan ice sheet. *J. Geol. Soc.*165 (1), 19–29.
- [61] Le Heron, D. P., Craig, J., Etienne, J. L., 2009. Ancient glaciations and hydrocarbon accumulations in North Africa and the Middle East. *Earth Sci. Rev.*93 (3), 47–76.
- [62] Legrand, P., 1981. Essai sur la paleogeographie du Silurien au Sahara algerien. *Compagnie Francaise des Petroles, Notes et Memoires*, Paris, 16: 9-24
- [63] Lehnert, O., Frýda, J., Buggisch, W., Munnecke, A., Nützel, A., Křiž, J., Manda, S., 2007. $\delta^{13}\text{C}$ records across the late Silurian Lau event: new data from middle palaeo-latitudes of northern peri-Gondwana (Prague Basin, Czech Republic). *Palaeogeography, Palaeoclimatology, Palaeoecology*, 245 (1-2), 227-244.
- [64] Lehnert, O., Männik, P., Joachimski, M. M., Calner, M., Frýda, J., 2010. Palaeoclimate perturbations before the Sheinwoodian glaciation: A trigger for extinctions during the 'Ireviken Event'. *Palaeogeography, Palaeoclimatology, Palaeoecology*, 296 (3-4), 320-331.
- [65] Lenz, A., Kozłowska, A., 2006. Graptolites from the lundgreni biozone (lower Homeric: Silurian), Arctic Islands, Canada: New species and supplementary material. *Journal of Paleontology*, 80 (4), 616-637.
- [66] Lewis, R., Ingraham, D., Percy, M., Williamson, J., Sawyer, W., Frantz, J., 2004. New evaluation techniques for gas shale reservoirs. In: *Reservoir Symposium*.
- [67] Loydell, D. K., Mannik, P., Nestor, V.2003. Integrated biostratigraphy of the lower Silurian of the Aizpute-41 core, Latvia. *Geological Magazine*, 140 (2), 205-229.
- [68] Loydell, D. K., Butcher, A., Fry´ da, J., Lüning, S., Fowler, M., 2009. Lower Silurian "hot shales" in Jordan: a new depositional model. *J. Pet. Geol.*32 (3), 261–270.
- [69] Loydell, D. K., Butcher, A., Frýda, J.2013. The middle Rhuddanian (lower Silurian) 'hot' shale of North Africa and Arabia: An atypical hydrocarbon source rock. *Palaeogeography, Palaeoclimatology, Palaeoecology*, 386, 233-256.
- [70] Lüning, S., Craig, J., Loydell, D. K., Štorch, P., Fitches, B., 2000a. Lower Silurian hot shales in North Africa and Arabia: regional distribution and depositional model. *Earth Sci. Rev.*49 (1), 121–200.
- [71] Lüning, S., Adamson, K., Craig, J., 2003. Frasnian organic-rich shales in North Africa: regional distribution and depositional model. *Geol. Soc., London, Special Publ.*207 (1), 165–184.
- [72] Macgregor, D. S., 1998. Giant fields, petroleum systems and exploration maturity of Algeria. *Geol. Soc., London, Special Publ.*132 (1), 79–96.
- [73] Massa, D., Beltrandi, M. (1975). Sédimentologie du Silurien de Libye Occidentale. In *IX Congrès international de sédimentologie (Vol.1, No.1, pp.13-1)*.
- [74] Massa, D., Jaeger, H., 1971. Données stratigraphiques sur le Silurien de l'Ouest de la Libye. In *Colloque Ordovicien-Silurien, Brest. Mémoires du Bureau des Recherches Géologiques et Minéralogiques (Vol.73, pp.313-321)*.
- [75] Massa, D., 1985. Un remarquable exemple de séries progradantes diachroniques, «Le Silurien de Tunisie Meridionale et de Libye Occidentale, Actes, du 1^{er} Congrès National des Sciences de la Terre, Tunis, pp.109–120, 11fig.

- [76] McAdams, N. E. B., Bancroft, A. M., Cramer, B. D., Witzke, B. J., 2017. Integrated carbon isotope and conodont biochemo-stratigraphy of the Silurian (Aeronian-Telychian) of the East-Central Iowa Basin, Iowa, USA. *Newsl. Stratigr.*50, 391–416.
- [77] McAdams, N. E., Cramer, B. D., Bancroft, A. M., Melchin, M. J., Devera, J. A., & Day, J. E., 2019. Integrated $\delta^{13}\text{C}_{\text{carb}}$, conodont, and graptolite biochemostratigraphy of the Silurian from the Illinois Basin and stratigraphic revision of the Bainbridge Group. *GSA Bulletin*, 131 (1-2), 335-352.
- [78] McLennan, S. M., Hemming, S., McDaniel, D. K., Hanson, G. N., 1993. Geochemical approaches to sedimentation, provenance, and tectonics. *Special Papers-Geological Society of America*, 21-21.
- [79] Melchin, M. J., Koren, T. N., Storch, P., 1998. Global diversity and survivorship patterns of Silurian graptoloids. In: Landing, E., Johnson, M. E. (Eds.), *Silurian Cycles: Linkages of Dynamic Stratigraphy with Atmospheric, Oceanic and Tectonic Changes*, New York State Museum Bulletin.491. pp.165–181.
- [80] Melchin, M. J., Mitchell, C. E., Holmden, C., Storch, P., 2013. Environmental changes in the late Ordovician early Silurian: Review and new insights from black shales and nitrogen isotopes. *Geol. Soc. Am. Bull.*125, 1635–1670.
- [81] Melchin, M. J., Sadler, P. M., Cramer, B. D. 2020. The Silurian Period. In *Geologic time scale 2020* (pp.695–732). Elsevier.
- [82] Memmi, L., Burolet, P. F., Viterbo, I., 1986. *Lexique stratigraphique de la Tunisie: première partie: Précambrien et Paléozoïque. Notes du Service géologique*, (53).
- [83] Meng, Q., Liu, Z., Bruch, A. A., Liu, R., Hu, F., 2012. Palaeoclimatic evolution during Eocene and its influence on oil shale mineralisation, Fushun basin, China. *J. Asian Earth Sci.*45, 95–105.
- [84] Moreau, J., 2011. The late ordovician deglaciation sequence of the SW murzuq Basin (Libya). *Basin Res.*23, 449-477.
- [85] Morton AC, Hallsworth C., 1994. Identifying provenance-specific features of detrital heavy mineral assemblages in sandstones. *Sedimentary Geology* 90 (3): 241-256.
- [86] Munnecke, A., Samtleben, C., Bickert, T., 2003. The Ireviken Event in the lower Silurian of Gotland, Sweden—relation to similar Palaeozoic and Proterozoic events. *Palaeogeogr. Palaeoclimatol. Palaeoecol.*195 (1), 99–124.
- [87] Noble, P. J., Zimmerman, M. K., Holmden, C., Lenz, A. C., 2005 Early Silurian (Wenlockian) $\delta^{13}\text{C}$ profiles from the Cape Phillips Formation, Arctic Canada and their relation to biotic events. *Canadian Journal of Earth Sciences* 42 (8), 1419-1430
- [88] Paris, F., Thusu, B., Rasul, S., Meinhold, G., Strogon, D., Howard, J. P., Whitham, A. G., 2012. Palynological and palynofacies analysis of early Silurian shales from borehole CDEG-2a in DorelGussa, eastern Murzuq Basin, Libya. *Rev. Palaeobot. Palynol.*174, 1–26.
- [89] Passey, Q. R., Bohacs, K. M., Esch, W. L., Klimentidis, R., & Sinha, S., 2010. From oil-prone source rock to gas-producing shale reservoir—geologic and petrophysical characterization of unconventional shale-gas reservoirs. In *International oil and gas conference and exhibition in China*. OnePetro.
- [90] Pearce TJ, Wray DS, Ratcliffe KT, Wright DK, Moscariello A (2005). Chemostratigraphy of the Upper Carboniferous Schooner Formation, southern North Sea. In: *Carboniferous hydrocarbon geology: the southern North Sea and surrounding onshore areas*. In: Collinson, J. D., D. J., Evans, D. W. Holliday, and N. S. Jones (eds.) *Yorkshire Geological Society, Occasional Publications series (7)*: 147-164.
- [91] Pettijohn FJ, Potter PE, Siever R (1987). *Sand and sandstone*. Springer Science & Business Media.
- [92] Rezouga, N., Soua, M., Alaya, S. B., Troudi, H., Saidi, M., Meskini, A., Zijlstra, H., 2012a. Assessment of an Unconventional Shale Resource Play: The Tannezuft “Hot Shales” in Ghadames Basin, South Tunisia. In: *11th SimposioBolivariano-ExploracionPetroleraen las CuencasSubandinas*.
- [93] Roser, B. P., &Korsch, R. J. (1988). Provenance signatures of sandstone-mudstone suites determined using discriminant function analysis of major-element data. *Chemical geology*, 67 (1-2), 119-139.
- [94] Ruban, D. A., Al-Husseini, M. I., Iwasaki, Y., 2007. Review of Middle East Paleozoic plate tectonics. *GeoArabia* 12 (3), 35–55.
- [95] Saltzman, M. R., 2001. Silurian $\delta^{13}\text{C}$ stratigraphy: a view from North America. *Geology* 29 (8), 671–674.
- [96] Saltzman, M. R., Thomas, E., 2012. Carbon isotope stratigraphy. In: *Geologic Time Scale 2012. vol 1 & 2*. pp.207–232.
- [97] Scotese, C. R., Boucot, A. J., McKerrow, W. S., 1999. Gondwanan palaeogeography and paleoclimatology. *J. Afr. Earth Sci.*28 (1), 99–114.
- [98] Scotese, C. R., 2004. A continental drift flipbook. *J. Geol.*112 (6), 729–741.
- [99] Soua, M., Zaghbib-Turki, D., Ben Jemia, H., Smaoui, J., Boukadi, A., 2011. Geochemical record of the Cenomanian–Turonian anoxic event in Tunisia: is it correlative and isochronous to the biotic signal? *Acta Geol. Sinica-English Ed.*85 (6), 1310–1335.
- [100] Soua, M., 2009. Gas from Shale Project-Regional Geology and Lithostratigraphy, 27p, ETAP Internal Report
- [101] Soua, M., 2013. First evidence of tunnel valley-like formation during the late Ordovician “subgalacial” period in Southern Tunisia Influence on the Jeffara sandstone reservoir quality. In: *18th Middle East Oil & Gas Show and Conference (MEOS, 2013)*, 21p.
- [102] Soua, M., 2014. Paleozoic oil/gas shale reservoirs in southern Tunisia: An overview. *Journal of African Earth Sciences*, 100, 450-492.
- [103] Soua, M., 2016. Chemostratigraphic approach: a tool to unravel the stratigraphy of the Permo-Carboniferous Unayzah Group and Basal Khuff Clastic Member, Central Saudi Arabia. *Saudi Aramco Journal of Technology*, 2016, 88-103.
- [104] Soua, M., 2019. Chemostratigraphy as a correlation tool for the permo-carboniferous unayzah group and basal khuffclastics member, central Saudi Arabia. in *AlAnzi, H. R., Rahmani, R. A., Steel, R. J., and Soliman, O. M. (AAPG), Eds., Siliciclastic reservoirs of the arabian plate: AAPG memoir 116: 83–102*.

- [105] Stampfli, G. M., Borel, G. D., 2002. A plate tectonic model for the Paleozoic and Mesozoic constrained by dynamic plate boundaries and restored synthetic oceanic isochrons. *Earth and Planetary science letters*, 196 (1-2), 17-33.
- [106] Štorch, P., Massa, D., 2006. Middle Llandovery (Aeronian) Graptolites of Western Murzuq Basin and Qarqaf Arch region, South West Libya. *Palaeontology* 49 (1), 83–112.
- [107] Štorch P., 1995 Biotic crisis and post-crisis recoveries recorded by Silurian planktonic graptolite faunas of the Barrandian Area (Czech Republic). *Geolines* 3: 59-70;
- [108] Sullivan, N. B., McLaughlin, P. I., Brett, C. E., Cramer, B. D., Kleffner, M. A., Thomka, J. R., Emsbo, P. 2016. Sequence boundaries and chronostratigraphic gaps in the Llandovery of Ohio and Kentucky: The record of early Silurian paleoceanographic events in east-central North America. *Geosphere*, 12 (6), 1813-1832.
- [109] Tang, Y. J., Jia, J. Y., Xie, X. D., 2002. Environment significance of clay minerals. *Earth Sci. Front.* 9, 337–344.
- [110] Tribouillard, N., Algeo, T. J., Lyons, T., Riboulleau, A., 2006. Trace metals as paleoredox and paleoproductivity proxies: an update. *Chem. Geol.* 232 (1), 12–32.
- [111] Troudi, H., Rezouga, N., Meskini, A., 2011. The Unconventional Gas Play in Tunisia Ghadames Basin Require a Certain Edge, Shale Gas Workshop-Oran, Algeria 27–29 February 2012.
- [112] Turgeon, S., Brumsack, H. J. 2006. Anoxic vs dysoxic events reflected in sediment geochemistry during the Cenomanian–Turonian Boundary Event (Cretaceous) in the Umbria–Marche Basin of central Italy. *Chemical Geology*, 234 (3-4), 321-339.
- [113] Vecoli, M., Riboulleau, A., Versteegh, G. J., 2009. Palynology, organic geochemistry and carbon isotope analysis of a latest Ordovician through Silurian clastic succession from borehole Tt1, Ghadamis Basin, southern Tunisia, North Africa: palaeoenvironmental interpretation. *Palaeogeogr. Palaeoclimatol. Palaeoecol.* 273 (3), 378–394.
- [114] Von Raumer, J., Stampfli, G., Borel, G., Bussy, F., 2002. Organization of pre-Variscan basement areas at the north-Gondwanan margin. *International Journal of Earth Sciences*, 91 (1), 35-52.
- [115] Wenekers, J. H. N., Wallace, F. K., Abugares, Y. I., 1996. The geology and hydrocarbons of the Sirt Basin: a synopsis. In: Salem, M. J., Mouzoughi, A. J., Hammuda, O. S. (Eds.), *The Geology of Sirt Basin: First Symposium on the Sedimentary Basin of Libya*, Tripoli, 10–13 October 1993, vol.1. Elsevier, Amsterdam, pp.3–58.
- [116] Worden, R. H., Morad, S. 1999. Clay minerals in sandstones: controls on formation, distribution and evolution. *Clay mineral cements in sandstones*, 1-41.
- [117] Young, R. A., 1993. The Rietveld Method. *International Union of Crystallography Monographs on Crystallography* 5. International Union of Crystallography; Oxford University Press, [Chester, England]: Oxford; New York, pp.308
- [118] Young, S. A., Benayoun, E., Kozik, N. P., Hints, O., Martma, T., Bergström, S. M., Owens, J. D., 2020. Marine redox variability from Baltica during extinction events in the latest Ordovician–early Silurian. *Palaeogeography, Palaeoclimatology, Palaeoecology*, 554, 109792.
- [119] Ziegler, P. A., Cloetingh, S., Guiraud, R., Stampfli, G. M., 2001. PeriTethyan Platforms: dynamics of rifting and basin inversion. In: Ziegler, P. A., Cavazza, W., Robertson, A. H. F., Crasquin-Soleau, S. (Eds.), *PeriTethys Mem.6: PeriTethyan Rift/Wrench Basins and Passive Margins. Mem. Mus. Natl. Hist. Nat., Paris, vol.186, P.9-49*